Journal of the
OPTICAL SOCIETY *of* AMERICA

VOLUME 29 NOVEMBER, 1939 NUMBER 11

A Thallous Sulphide Photo-e.m.f. Cell

FOSTER C. NIX AND ARNOLD W. TREPTOW
Bell Telephone Laboratories, New York, New York

(Received August 19, 1939)

A photo-e.m.f. effect is observed in Tl_2S produced by partial sulphurization of a thallium disk or of an evaporated thallium layer. The photosensitivity is observed to be as high as $6000 \cdot 10^{-6}$ ampere/lumen. Both open-circuit-voltage and short-circuit-current are observed in some cells to be directly proportional to the incident light intensity at all temperatures. In other cells, especially those displaying high photo-response, the open-circuit-voltage and short-circuit-current tend to saturate at high light intensities. The spectral photosensitivity curve possesses a maximum at 9800A±200A with long and short wave thresholds at 15,000 and 6500A, respectively. The short-circuit-current *increases* with *decreasing* temperature down to about −45°C and then decreases continuously down to −180°C. The position of the maximum varies somewhat from cell to cell. The photoelectric output of the cells when measured as a function of frequency of interruption of the incident light displays a recession of 75 percent at 20,000 cycles.

IN recent years a number of investigators have reported studies on the provoking of a photo-electric current by light, without the aid of an external source of potential, in systems utilizing photoconducting materials, e.g., Cu_2O and selenium. The various observed phenomena can be divided into two general classes which have been designated as barrier-layer (*sperrschicht*) or rectifier, and crystal photo-effects. In the so-called barrier-layer system the observed photo-effect is supposed to arise only when a transition layer (barrier-layer) about 10^{-6} cm thick exists between the photosensitive semiconductor and an adjoining metallic electrode. The presence of this transition layer is also supposed to provoke a rectification of an electric current, i.e., electrons can flow from the metallic electrode through the barrier-layer into the semiconductor more freely than they flow in the opposite direction. This condition is thought to arise by virtue of the differences in distribution of electron energies in the metal and semiconductor. According to the theory of Frenkel and Joffè[1] one is led to expect a disappearance of the photo-e.m.f. effect simultaneously with the disappearance of the rectification. The barrier-layer effect has been observed in the cells utilizing Cu_2O and selenium as the photosensitive semiconductor. The crystal photo-effect has been observed in such materials as diamond,[2] zincblende[3] (ZnS), rocksalt[4] (NaCl) and cuprite (Cu_2O).[5]

The Cu_2O photo-e.m.f. cells[6] have been divided into two general classes depending on the location of the hypothetical barrier-layer. In the earlier cells, produced by partially oxidizing copper plates to form a thin layer of Cu_2O on the

[1] J. Frenkel and A. Joffè, Physik. Zeits. d. Sowjetunion **1**, 60 (1932).
[2] R. Robertson, J. J. Fox, and A. E. Martin, Nature **129**, 579 (1932); Phil. Trans. Roy. Soc. London **A232**, 463 (1934).
[3] H. Dember, Naturwiss. **20**, 758 (1932).
[4] S. Pelz, Naturwiss. **21**, 517 (1933).
[5] H. Dember, Physik. Zeits. **32**, 554 (1931).
[6] F. C. Nix, Rev. Mod. Phys. **4**, 723 (1932).

BOSTON UNIVERSITY
COLLEGE OF LIBERAL ARTS
LIBRARY

copper, the barrier-layer is assumed to be the transition zone between the metal and the oxide. On illumination of the Cu_2O surface photoelectrons flow from the Cu_2O through the barrier-layer into the copper base. On the other hand the thermal electrons, under the influence of an applied electric potential, flow more easily from the copper base through the barrier-layer to the Cu_2O. Schottky and Duhme[7] then showed that bombarding one surface of a massive Cu_2O plate with electrons or ions, or etching the surface with suitable reagents, produced a barrier-layer on the surface. When subsequently coated with a metal by sputtering or evaporation, to form what we shall designate as an auxiliary electrode, the layer gave rise to a rectification and a photo-e.m.f. effect on illumination of the electrode. It is only necessary that the electrode on the reverse side of the Cu_2O plate form an ohmic contact. The direction of favored electron flow or low resistance for the thermal electrons driven by an external potential is from the auxiliary electrode through the barrier-layer to the Cu_2O plate. The photoelectrons flow from the Cu_2O through the barrier-layer into the auxiliary electrode. The cells produced by the partial oxidation of a copper plate, i.e., where the barrier-layer is situated between the Cu_2O and the copper base, have been designated as back-wall cells, whereas the cells formed by treatment of one surface of massive Cu_2O slab are called front-wall cells. In one important respect the two types are essentially the same, i.e., in both cells the photoelectrons flow from the Cu_2O through the barrier-layer.

In the Cu_2O front-wall[8] effect the photosensitive spectral response is a simple bell-like curve with a maximum at *ca.* 5400A, and with the long and short wave thresholds at *ca.* 6500A and 4500A, respectively. The back-wall cells[9] have a maximum identical in position to the maximum for the photoconductivity of Cu_2O, i.e., at *ca.* 6350A with some sensitivity extending into the infra-red, whereas the short wave threshold occurs at *ca.* 6000A. This rapid decrease of photo-response on the short wave side of the maximum is thought to be due to the filtering effect of the Cu_2O in front of the barrier-layer.

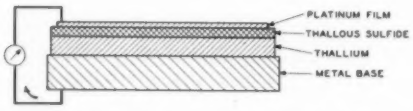

FIG. 1. A schematic diagram of the Tl_2S photo-e.m.f. cell. Arrow indicates the direction of flow of the photoelectrons.

In the following we shall describe and discuss the method of production and characteristics of a new photo-e.m.f. cell[10] of Tl_2S.* We shall also show wherein the existing theories of photo-e.m.f. effects completely fail to explain the observed phenomenon.

The cell consists essentially of a partially sulphurized thallium layer on top of which is sputtered a thin semitransparent conducting film of platinum or gold. The thallium film is obtained either by evaporation onto a metallic disk, e.g., copper or nickel, which serves only as a conducting mechanical support and plays no role in the observed photo-effect, or simply by using a disk of thallium. On exposure to the atmosphere, the thallium film or disk suffers a surface oxidation, which is subsequently removed by heating in the evacuated tube used in the sulphurization process. The free thallium surface obtained by heating to *ca.* 280°C possesses the metallic luster characteristic of a clean metallic surface. These surfaces are then exposed to a self-sustaining glow discharge in dry H_2S gas or the sulphur vapor obtained by heating flowers of sulphur, in order to obtain the desired degree of sulphurization. These methods of obtaining the sulphur were selected because of ease in maintaining a constant and uniform sulphur concentration at the surfaces to be sulphurized, permitting sulphurization to continue for accurately controlled periods of time under reproducible conditions. After sulphurization the evacuated system is allowed to cool to room temperature at which time the unit is removed and receives a thin auxiliary electrode of sputtered platinum or gold. This semitransparent conducting auxiliary electrode serves as the front electrode, and the metallic supporting disk constitutes the back

[7] E. Duhme and W. Schottky, Naturwiss. **18**, 735 (1930).
[8] Campbell and Ritchie, *Photoelectric Cells* (Pitman & Sons, Ltd., 1934).
[9] M. Dubar, Comptes rendus **193**, 659 (1931).
[10] B. Kolomiez, (Comptes rendus (Doklady) de l'Academie des Sciences d l'U. R. S. S. **14** (1938)) has recently published a brief note concerning a similar cell.
* This cell is still considered a piece of laboratory apparatus and is not available for commercial distribution.

electrode. Fig. 1 depicts diagrammatically the structure of the complete cell. The arrow indicates direction of flow of the photoelectrons. The *direction* of *flow of the photoelectrons* was always *from the* Tl_2S *into the free thallium metal* from which the Tl_2S was obtained by sulphurization.

Measurements on the cells produced by sulphurization in the H_2S glow discharge of the evaporated thallium metal, possessing photosensitivities from $300–600 \cdot 10^{-6}$ ampere/lumen, at temperatures varying from room temperature down to liquid-air temperature show the short-circuit-current and open-circuit-voltage to be rigorously proportional to incident light intensity at all temperatures. Fig. 2 depicts the characteristics of one such cell at −180°C. The curves are typical of results obtained on a large number of cells possessing photosensitivities less than $700 \cdot 10^{-6}$ ampere/lumen. These results stand in rather strong contrast with those reported for most of the Cu_2O[11] and selenium barrier-layer cells also possessing similar photosensitivities, in which the short-circuit-current is proportional to incident light intensity, whereas the open-circuit voltage is proportional only at very low light intensities and tends to saturate with increasing light intensity.

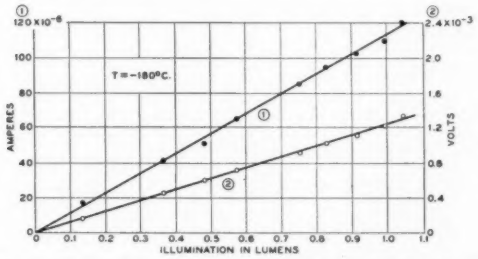

FIG. 2. Short-circuit current, (1) and open-circuit voltage, (2) *vs.* light intensity of a cell at −180°C.

Figure 3 shows how the characteristic of current *vs.* light intensity at room temperature for these cells is affected by the insertion of various resistances in the external circuit. It can be seen that their effect is simply to decrease the current without in any way changing the nature of the characteristic. This, however, was to be expected in light of the fact that *both* short-circuit current

[11] O. v. Auwers and H. Kerschbaum, Ann. d. Physik **7**, 129 (1930).

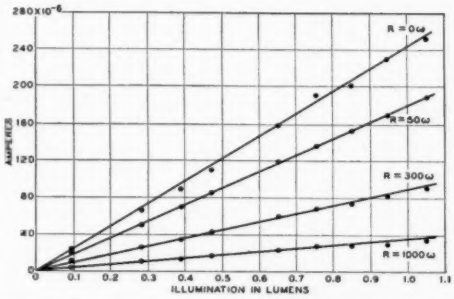

FIG. 3. Photo-current *vs.* light intensity characteristics with external series resistances of $R=0$, 50, 300 and 1000 ohms in the measuring circuit.

and open-circuit voltage were found to be directly proportional to the incident light intensity. In the case of selenium[12] and Cu_2O photo-e.m.f. cells, the insertion of resistances had shown a tendency to produce saturation of current with light intensity.

In the latter stage of this research, technique was improved permitting us to obtain cells possessing a photo-response as high as $6000 \cdot 10^{-6}$ ampere/lumen although the average cell gave a photo-response between $3000–4000 \cdot 10^{-6}$ ampere/lumen. The technique yielding the most reproducible results consisted essentially in the sulphurization of thermally cleaned thallium disks by sulphur vapor obtained by the heating of flowers of sulphur.

The open-circuit voltage and short-circuit current *vs.* light intensity characteristics of cells possessing a photo-response from $1500–6000 \cdot 10^{-6}$ ampere/lumen display drastically different features from the lower sensitivity cells depicted in Figs. 2 and 3. Typical curves for the short-circuit current and open-circuit voltage *vs.* light intensity for these cells are given in Figs. 4 and 5, respectively. We note a slight tendency for the short-circuit current to saturate with light intensity, whereas, the open-circuit voltage *vs.* light intensity curve displays a marked tendency to saturate at luminous flux densities as low as 0.35 lumen. These tendencies to saturate with light intensity for both the short-circuit current and open-circuit voltage vary somewhat from cell to cell. The resistance of the cells varied from 20 to 1000 ohms, and did not suffer an appreciable change on illumination.

[12] L. Bergmann, Physik. Zeits. **33**, 513 (1932).

The short-circuit current yield was measured with a meter possessing a resistance of only 1.2 ohms. These measurements were made by exposure to the general radiation from an incandescent tungsten lamp at a color temperature of 2848°K. In general, the photo-response yield of a photoelectric cell is stated in terms of units of luminous flux, which necessarily implies response to visible light. As is to be seen from Fig. 7 the Tl_2S photo-e.m.f. cell only possesses a

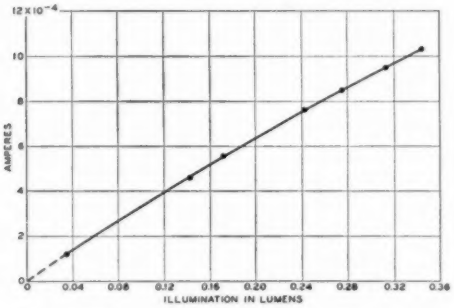

FIG. 4. Short-circuit current *vs.* light intensity.

slight photo-response to visible light which means that, rigorously, a statement of yield with reference to lumens is meaningless. Nevertheless, we have stated the short-circuit current yield in terms of current per lumen of incident light so as to permit a direct comparison to be made with other cells as measured with similar light sources (e.g., tungsten lamp). The short-circuit current yield of Cu_2O front- and back-wall cells is $150 \cdot 10^{-6}$ and $15 \cdot 10^{-6}$ ampere/lumen, respectively, whereas the yield of a selenium photo-e.m.f. cell is somewhat greater, *ca.* $450 \cdot 10^{-6}$ ampere/lumen.

Careful measurements were made in order to ascertain whether rectification occurred in the cells such as is found to be the case with most Cu_2O and selenium photo-e.m.f. cells. In a large number of measurements made at room temperature and at various temperatures down to that of liquid air *no evidence of a rectification was observed*. These results, along with others reported by Borissow, Sinelnikow and Walther,[13] Wood,[14] on Cu_2O cells and by Roy-Pochon[15] on selenium cells, indicate that the rectification phenomenon is not to be considered as a necessary accompaniment of the photo-e.m.f. effect. The temperature coefficient of the dark resistance was found to be extremely small: the dark resistance increases only by a factor of two on passing from room temperature down to that of liquid air.

The short-circuit current output as a function of temperature is depicted in Fig. 6 as measured by exposure to the general radiation of an incandescent tungsten lamp. This characteristic is not to be considered as an accurate quantitative measure of the photo-response as a function of temperature, since it fails to take into consideration the shift in absorption and spectral photo-response domains with temperature usually observed in photo-conducting materials. The photo-response was observed to *increase* with *decreasing* temperature down to *about* $-45°C$ at which point a further decrease in temperature provoked a *decrease* in the photo-response. The photosensitivity continuously decreased from this maximum at $-45°C$ down to $-180°C$.

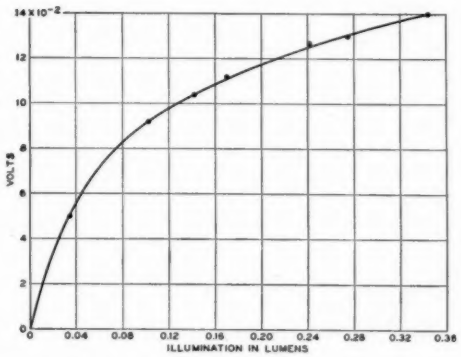

FIG. 5. Open-circuit voltage *vs.* light intensity.

The position of the maximum varied somewhat from cell to cell ($-5°C$ to $-45°C$), but the general shape of the curves was the same for all. The measurements were made in a tube similar to that used by Nix[16] in photoconductivity measurements on red HgI_2. The cell was mounted on the end of a re-entrant copper tube in an evacuated glass vessel with flat Pyrex glass windows permitting the cell to be cooled and

[13] M. Borissow, C. Sinelnikow and A. Walther, Physik. Zeits. d. Sowjetunion **3**, 146 (1933).
[14] L. A. Wood, Rev. Sci. Inst. **6**, 196 (1935).
[15] Mme. Roy-Pochon, Comptes rendus **198**, 2083 (1934).
[16] F. C. Nix, Phys. Rev. **47**, 72 (1935).

maintained at several temperatures from 25° to −180°C.

When sufficient care is taken to avoid undue heating of the cells, by such precautions as the insertion of a water cell in the optical train, the short-circuit current output was found to be *independent* of the *time* of *illumination* over a period of several hours. In cases where the incident light heated the cell, a decrease of photo-response was observed, as was to be

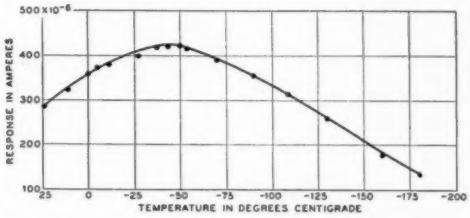

FIG. 6. Short-circuit current response *vs.* temperature.

expected from the temperature coefficient of the photo-response at room temperature.

Spectral response measurements on a number of cells, when plotted on an equi-energy basis, display a pronounced single bell-like maximum at 9800A±200A with the long and short wave thresholds in the neighborhood of 15,000 and 6500A, respectively. A typical spectral response curve is given in Fig. 7. A representative transmission curve of Tl_2S film on glass is also included in order to show the relationship between optical absorption and the spectral photo-response. It is to be noted that the maximum spectral photoelectric response occurs near the edge of the absorption band. This general relationship was also observed for the back-wall Cu_2O cells. It is also of interest to note that the cells only possess a slight photo-response in the visible spectrum, whereas the Case Thalofide photoconducting cell, as reported by Coblentz,[17] displayed an appreciable photo-response at 6000A. This same general relationship is also known to exist between the photoconductivity spectral domain of Cu_2O and the spectral response of the back-wall Cu_2O effect. This lack of photoelectric response in the more highly optically absorbent region for both Tl_2S and back-

[17] W. W. Coblentz, Sci. Paper, Nat. Bur. Standards, No. 380 (1920).

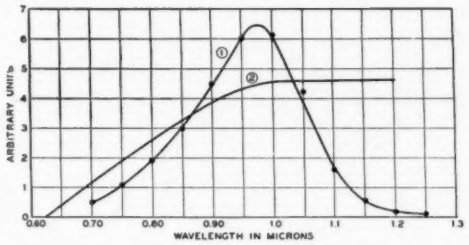

FIG. 7. (1) A typical equi-energy spectral response curve of a Tl_2S photo-e.m.f. cell. (2) Optical transmission curve for a thin film of Tl_2S on glass.

wall Cu_2O cells is doubtless due to a filtering effect of the photosensitive material.

Figure 8 gives the photoelectric output, as measured with a resistance-capacity-coupled amplifier, of a Tl_2S photo-e.m.f. cell as a function of the frequency of interruption of the incident light, up to 20,000 cycles per second. The load resistance of the cell was 2000 ohms. The data supplied by the producers of the selenium photronic cell is also given in Fig. 8 in order to permit a direct comparison to be made between the two cells. As is to be seen from the two curves, the Tl_2S photo-e.m.f. cell possesses vastly superior properties when used at high frequencies.

The finished cells with appropriate contacts to the platinum film and the back metallic disk were mounted in various atmospheres and observed over a period of three years for stability. The cells were sealed in well-evacuated tubes or tubes containing ordinary dry air, nitrogen and other gases at different pressures. Some cells were also mounted in containers which were sealed with various synthetic resins to prevent water vapor from being in direct contact with the cell itself. Regardless of the system used most cells deteriorated substantially over periods varying from several days to two or more years. In some cases cells retain some 85 percent of their original photosensitivity after two years of observation. Cells which deteriorated when sealed in evacuated tubes or in tubes containing N_2, H_2, He, etc. could be restored to their original sensitivity on exposure to oxygen or air. We are unable to explain these factors which control the stability of the cells.

The various theories put forward to explain the two observed photo-e.m.f. effects completely

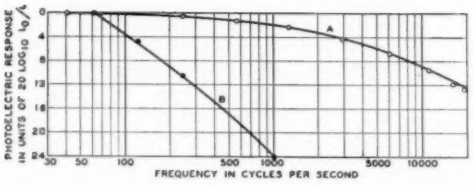

FIG. 8. Curves depicting photoelectric response *vs.* frequency of interruption of the incident light of (*A*) a Tl_2S photo-e.m.f. cell and (b) a photronic cell (a selenium photo-e.m.f. cell.)

fail to explain our results on Tl_2S photo-e.m.f. cells. The Frenkel-Joffè[1] theory of rectification and barrier-layer photo-e.m.f. effects in Cu_2O explicitly connects the photo-effect with the rectification of an electric current. They state, "This explains the fact that the contact photo-electric effect vanishes in the case of good contacts simultaneously with rectification." The absence of all indications of a rectification of an electric current by our cells clearly shows the inadequacy of the Frenkel-Joffè theory to explain the observed effect. It has also been reported that large photo-e.m.f. effects are observed in Cu_2O cells with no or only a slight indication of unipolar conduction. Roy-Pochon[15] states she observed that 1 percent of a large number of selenium photo-e.m.f. cells failed to possess any indication of rectifying effects. It thus appears that rectification is not essential to the photo-e.m.f. effect. Joffè[18] attempts to discredit the lack of rectification in Cu_2O cells as evidence against the Frenkel-Joffè[18] theory by assuming the barrier-layer in these cases to possess a low specific resistance compared to the body resistance of the Cu_2O thereby masking the effect provoked by the non-ohmic properties of the barrier-layer. The writers cannot concede this argument to be tenable in the light of our results, for in some cases the total resistance of the cell was found to be as low as 20 ohms. The theoretical attempts to explain the so-called crystal photo-e.m.f. effect observed by Dember, and others in single crystals of the mineral cuprite also fail when applied to our observations. These theories all require a saturation tendency of the open-circuit voltage *vs.* light intensity which is inconsistent with the direct proportionality with incident light intensity as observed by us on many cells.

The writers are indebted to Mr. R. Rulison for assistance in the experimental work and to Mr. M. W. Baldwin, Jr., for making the photo-response *vs.* frequency of interruption of light measurements.

[18] A. F. Joffè, *Semi-Conducteurs Electroniques* (Hermann & Cie, Paris, 1935).

Fundus Photography without Cycloplegics

KATHYRN LOUISE STONE
College of Optometry, Ohio State University, Columbus, Ohio

AND

M. L. POOL
Department of Physics, Ohio State University, Columbus, Ohio

(Received August 28, 1939)

With the use of the new H6 water-cooled 1000-watt mercury arc lamp, two Polaroids, a new fast film of Weston rating 140, and a simple optical system photographs of the fundus of the eye have easily been made without the use of drugs that dilate the pupil.

INTRODUCTION

PHOTOGRAPHS of the fundus of the living human eye have been made for many years and have been of the utmost value in the diagnosis and prognostic observation of many affections of the eye. This photographic aid, however, has been limited to the oculist and ophthalmologist. They alone are permitted to use cycloplegics which dilate the pupil, and pupillary dilation is essential for the satisfactory operation of retinal cameras now available. Of these the Nordenson retinal camera is used almost universally.

It is the purpose of this paper to describe a simple camera unit which is relatively inexpensive, eliminates the necessity for using cycloplegics and removes the customary corneal reflex.

OPTICAL ARRANGEMENT

Figure 1 shows a schematic diagram of the optical system used in illuminating the fundus of the eye. The light from the source S_1 is condensed by the lens L_1 onto the variable slit *SL*. This light then passes through the shutter *SH* and into the lens L_2 which focuses the light in the pupil of the eye at E_1. The light passes on into the eye and merely illuminates the fundus. M_1 and M_2 are plane and nearly transparent mirrors made of thin pieces of good quality glass. The source S_2 is placed at such a position that its image produced by the lens L_2 is also at E_1. The source S_3 is placed at the primary focus of the lens L_4. The distance from E_1 to E_2 is the interpupillary distance.

Figure 2 shows a schematic diagram of the optical system involved in the emission of the

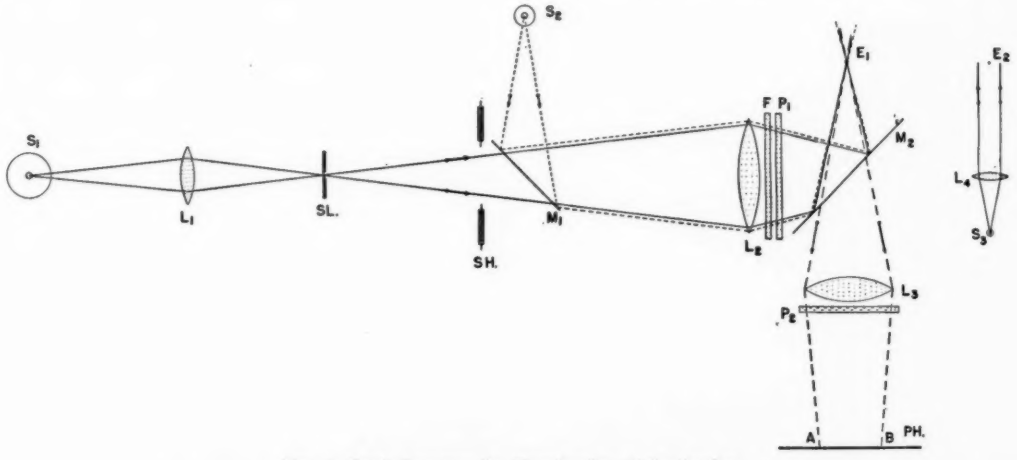

FIG. 1. Optical system for illumination of the fundus.

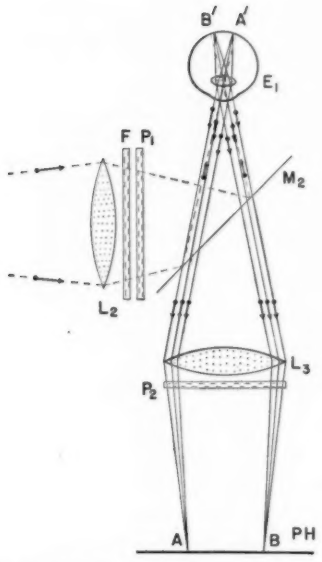

FIG. 2. Optical system for light emitted from the fundus.

light from the illuminated fundus. Since the points A' and B' are both in the primary focal plane of the compound lens system of the eye, the light leaving these points and defined by the iris consists of two diverging beams of parallel light. A portion of the camera lens L_3 intercepts these two beams and focuses them on the photographic plate PH at the points A and B, respectively. This lens L_3 should have a large aperture in order to be able to receive light from widely separated portions of the fundus and a focal length as short as possible in order to reduce the size of the image and thus increase the speed of the camera. The focal lengths of the lenses L_1 and L_2 are 35 mm and 60 mm, respectively. For the lens L_3 the following have been used: focal lengths 75, 50 and 25 mm with speeds, respectively, $f:1.8$, $f:1.5$ and $f:1.3$.

SOURCES, FILTERS, POLAROIDS AND FILM

For the primary source S_1, the new high intensity type H6 1000-watt water-cooled mercury arc lamp has been used with excellent satisfaction.[1] Its very high intrinsic intensity, the narrow capillary source and the spectral energy distribution are particularly suited for the photographic requirements in this work. The contrast on the photographic film between the blood vessels and the surrounding medium that composes the fundus of the eye is brought out best with green light illumination. The H6 arc lamp fortunately emits a large percent of its total radiation in the yellow-green line, 5461A.[2]

In comparison with other types of mercury arcs there is from this new lamp a very pronounced continuous spectral background. The energy in this background, nevertheless, is small compared with the energy in the principal mercury lines. The principal lines 4358, 4047 and 3660A should not be allowed to enter the eye and may be removed by filters. The Jena filter GG11 or the Wratten filters K-2, G or the monochromatic No. 77 have been found about equally satisfactory. The circulating water, used in cooling, absorbs about 90 percent of the infra-red radiation.[3]

For a very simple light source, although not quite as satisfactory as the H6 lamp, the new high efficiency tungsten coiled filament lamp has been used.[4] This 120-volt, 60-watt lamp in clear glass with the C6 filament is used at about 210 volts. Since the filament is very small and straight it can be sharply focused on the slit S_1 and a large portion of the radiant output energy thus utilized. It is now necessary to be more careful in the selection of the filters. The Jena filters BG 19 and GG 11, used together, have been found adequate.

P_1 in Fig. 1 is a Polaroid which is rotated in such a way that the light from the slit S_1 is polarized in a plane perpendicular to the plane of the figure. Light reflected from the cornea remains, for the most part, polarized and that reflected from the fundus is depolarized. Since the intensity of the light reflected from the cornea is comparable to that from the fundus, it is therefore necessary to rotate the Polaroid P_2 in such a way as to cut out all light polarized in the original plane. Consequently, only depolarized radiation from the fundus gets through the second Polaroid and onto the photographic film.

The new commercial Eastman Tri-X panchromatic film has been found more satisfactory

[1] Gen. Elec. Rev. **42**, 46 (1939).

[2] L. J. Buttolph, J. Opt. Soc. Am. **29**, 124 (1939).

[3] E. B. Noel and R. E. Farnham, J. Soc. Mot. Pict. Eng. **31**, 221 (1938).

[4] E. W. Beggs, J. Opt. Soc. Am. **29**, 117 (1939).

than any other of a number of films and professional plates tried. This film has a Weston speed rating of 140 when developed in DK 60a.

Results

In taking a picture of the fundus the procedure is first to close the shutter *SH* and turn on the source S_2 which is weak and can be varied to just visibility. The eye in position E_1 then sees a faint general red glow when adjustments are correct. The only purpose of this weak source is to make it possible for the patient to put his eye, the one to be photographed, in the proper position while it is dark adapted. The patient as well as the complete apparatus is housed in a darkened booth. Should the light from the strong source S_1 (about 10,000 times as strong as the source S_2) be admitted through the shutter *SH* for the purpose of making preliminary adjustments, the iris of the patient would contract to so small a size that subsequent photography would be impossible. If the iris were prevented from contracting by the use of cycloplegics, then the source S_2 would obviously be unnecessary and the source S_1 could be used in making the preliminary adjustments.

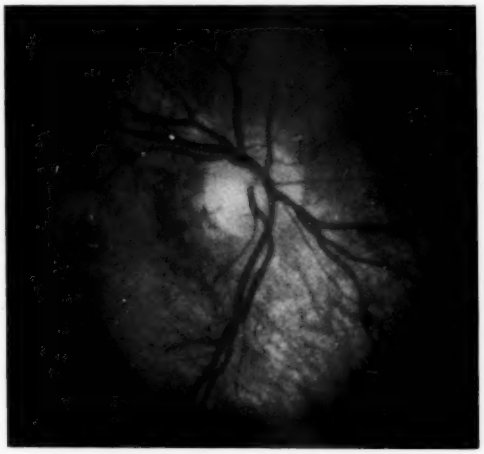

Fig. 3. Photograph of the fundus.

Since the amount of light from the weak source S_2 falling upon the fundus is just enough to give to the patient the sensation of light, the amount of light reflected back from this faintly illuminated fundus and onto the photographic film is indeed very feeble. Consequently, it is not necessary to use a shutter on the camera lens itself.

The eye in position E_2 is relaxed and sees at infinity the virtual image of the source S_3. Since the eye at position E_1 is therefore also relaxed, it is only necessary to set the camera unit to focus parallel light in order to get a sharp picture of the fundus. When these preliminary adjustments have been made, the shutter *SH* is then opened for a predetermined short length of time to allow the light from the very strong primary source S_1 to illuminate the fundus.

Figure 3 is a picture of the fundus obtained with the H6 arc source and the GG 11 filter. The pupil was only moderately dark adapted, and the exposure time was 1/10 sec. In the picture can be seen the whitish optic nerve head or optic disk, the retinal blood vessels, both arteries and veins, and some choroidal vessels dimly in the background. One notices no abnormalities and so concludes that this is a normal fundus.

When the C6 filament lamp is used it is necessary to lengthen the exposure time to at least 1/5 sec.; in addition the excellent photographic detail and contrast is always somewhat lacking. Since eye movements are frequently noticeable it is advantageous to keep the exposure time as short as possible.

Some progress has already been made with using colored 35-mm films. Since these films have an appreciably slower emulsion speed, a wider slit and the full intensity of the H6 arc source must be used. Report on this work will be reserved to a later date.

Wide Range Intensity Measurements in Photoelectric Spectrophotometry

WALTER C. BOSCH AND BARREMORE B. BROWN
Department of Physics, Tulane University, New Orleans, Louisiana

(Received September 21, 1939)

Methods of measuring intensity in photoelectric spectrophotometry are discussed, and conditions for maximum reasonably precise utilization of amplifier galvanometer response are experimentally investigated. For a spectrophotometer having four light sensitivity ranges, differing by approximate multiples of ten, it is shown that, if proper grid bias is used on each range, deflection is proportional to incident light intensity within ±0.5 percent for applied grid potentials from 0 to 0.3 v. With a suitably selected galvanometer system, deflections measure light intensities from 1.0 to 10^6 arbitrary units over the whole response range of the instrument. It is also shown that for applied grid potentials from 0 to 0.5 v, the deviation from linearity does not exceed ±1.5 percent.

INTRODUCTION

IN a photoelectric spectrophotometer utilizing electrometer tube amplification, such as that described by Hogness and his colleagues,[1] two methods are available for obtaining a measure of the intensity of radiation incident on the photocell. In the first of these methods, the deflections of the plate galvanometer are accepted as proportional to the radiation intensity. In the second procedure, the changes of conductance of the photo-cell from the dark level are determined by a null method, the amplifier serving only as a sensitive null indicator. The equation for computation of change of conductance, ΔC, is:

$$\Delta C=\frac{E_n}{(E-E_n)R}, \tag{1}$$

where E_n is the potential required to balance out the potential drop, due to photo-current, on the grid resistance, R, in series with the photocell, and E is the total potential in the photo-cell circuit.

The second of these two methods is the more accurate over a wide range of intensity values, but is rather tedious to apply. For many problems it is far more convenient to use the deflection method. In the instrument mentioned above,[1] for example, deflections are used, and good precision in securing absorption data for solutions has been obtained by limiting the applied potential on the amplifier control grid to approximately 15 mv.

It was the purpose of the present investigation to determine the conditions for maximum precision utilization of the deflection method in a photoelectric spectrophotometer responsive to a wide range of light intensity. In this type of instrument, several sensitivity ranges are obtained by using appropriate values of grid resistance in series with the photo-cell. (A switching arrangement for convenient range changing is described by Strong.[2]) In the method used herein, changes of photo-cell conductance, computed from Eq. (1), are accepted as proportional to the intensity of the incident radiation and compared with the corresponding galvanometer deflections. For each sensitivity setting, circuit conditions for a maximum range of deflection-intensity proportionality are determined. The relation between deflection, d, and change of conductance is:

$$d=\left[\frac{AE}{(1+\Delta C\cdot R)k}\right]\Delta C, \tag{2}$$

where the symbols not previously defined are A, the current amplification factor, and k, the galvanometer constant. It is obvious that the bracketed factor of Eq. (2) must remain essentially constant in any operation range. When various resistance values R_1, R_2, etc., are used, Eq. (2) takes the form:

$$\frac{\Delta C}{d}=K_1;\quad \frac{\Delta C}{d}=K_2,\quad \text{etc.} \tag{3}$$

[1] T. R. Hogness, F. P. Zscheile, Jr. and A. E. Sidwell, J. Phys. Chem. **41**, 379 (1937).

[2] J. Strong, *Procedures in Experimental Physics* (Prentice-Hall, 1938), p. 423.

Apparatus

The spectrophotometer used, similar in some essential parts to that described by the workers[1] mentioned above, was designed for use in general spectrophotometric work. For mechanical stability and accurate tracking of auxiliary equipment, the optical system is mounted on a heavy lathe bed. The dispersing device is a Bausch and Lomb quartz single monochromator with wavelength range 2000 to 8000A. Energy from its exit slit is received on a G-M 1038A Cs-O, gas-filled, emission type quartz photo-cell connected to a DuBridge-Brown[3] balanced amplifier as shown in Fig. 1. The amplifier galvanometer, mounted on a modified Julius suspension and connected to a decimal Ayrton shunt, is a Leeds and Northrup Type R used with a 50-cm scale at a distance of 3.5 meters. Its full sensitivity under conditions of use is 2.26×10^{-10} amp./mm.

A standardized Leeds and Northrup potentiometer, P_1, range 0 to 2.3 v, and a voltage divider, P_2, are connected in series in the grid circuit of the amplifier in the place of the usual single calibrating potentiometer. P_1 is used in null measurements. P_2 serves to bias the amplifier grid to a suitable value for galvanometer response linearity and its use will be discussed below.

Four light sensitivity ranges, differing by approximate multiples of ten are available. To obtain these ranges, S. S. White resistors of values (in ohms) 10^8, 1.08×10^9, 9.3×10^9, and 10^{11} are connected, as needed, at R_1 or R_2 in the photo-cell circuit.

Light sources used in calibration are, principally, the quartz mercury arc and various incandescents. These are operated on d.c. generators or storage batteries to secure constancy of light output. When sources operating on a.c. are used, a constant voltage transformer is introduced into the circuit.

Calibration Procedure and Results

In all utilizations of the instrument described, the flow of photo-current through the grid resistor applies a negative increment to the grid bias, and the amplifier is adjusted to the balance level.[3]

[3] L. A. DuBridge and H. Brown, Rev. Sci. Inst. **4**, 532 (1933).

In calibrating any given sensitivity range, the monochromator, with slits adjusted to 0.1 mm, is set for the selected spectral region, and potentiometers P_1 and P_2 are set to zero. By adjusting the position, aperture, or intensity of the light source, or by focus changes, the intensity of light on the photo-cell is changed through a range of values. The intensity values selected result in the application of grid potential increments from 0.001 to 0.5 v. For each intensity, the deflection is read and the nulling voltage determined by utilizing potentiometer P_1. Using Eq. (1), the changes of conductance of the photocell are determined, and the ratios $\Delta C/d$ computed and tested for constancy as suggested in Eq. (3). In general, the ratios show large deviations from constancy.

An inspection of the bracketed factor of Eq. (2) shows that E, k, and R are constants. The expression, $(1+\Delta C\cdot R)$, does contribute to nonlinearity as discussed, from a slightly different approach, by Zworykin and Wilson.[4] However, it can be shown that, for any value of R, and for applied grid potentials up to 0.5 v, $(1+\Delta C\cdot R)$ has a maximum value of approximately 1.005. It is obvious that the large variations from constancy referred to above are due to variations in the current amplification factor, A.

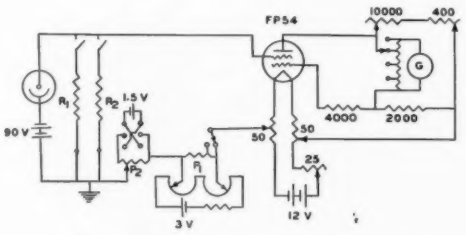

Fig. 1. Photo-cell-amplifier circuit of the spectrophotometer.

To determine the approximate voltage range in which A is constant, for any given value of R, increments of potential up to 1.5 v, positive and negative, are applied to the grid of the amplifier after the circuit is balanced. The values of potential and deflection at each setting are used with k and R to compute the value of A. The values of A are then plotted against the applied

[4] V. K. Zworykin and E. D. Wilson, *Photocells and Their Application* (Wiley, 1934), p. 157 *et seq.*

grid potentials. A set of such curves for the four resistance values used is shown in Fig. 2. Each of these curves has about the same general shape, with a plateau ranging about 0.3 v in length. The plateau may be considered as extending an additional 0.1 v in either direction (a total length of 0.5 v) with only small changes in the value of A. It will also be noted that, with the exception of the 1.08×10^9 curve, the plateaus do not extend through the zero (or balance)

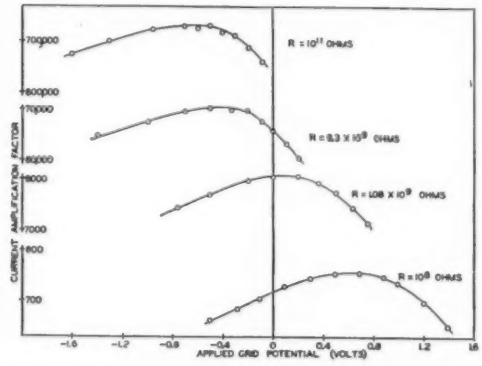

FIG. 2. Curves used in approximating proper grid bias values for linear galvanometer response on the four sensitivity ranges of the instrument.

level. The curves suggest that, for each value of R, there is a grid potential setting from which changes of grid potential up to 0.5 v will not materially affect the constancy of A. For any given value of R, the constant voltage, positive or negative, required to bias the amplifier to the beginning of the linear range, is estimated from the appropriate curve. This voltage is then locked in on potentiometer P_2, and the galvanometer is brought back to zero by adjusting the plate circuit controls of the amplifier. Readings, either by null or deflection methods, may then proceed in the usual manner.

To determine more precisely the bias required for any given range, voltage sensitivity data is taken with the estimated bias value applied in the circuit. Minor adjustments of the bias potential are then made until the voltage sensitivity is essentially constant over the selected voltage range. Finally, using a given spectral region, usually 2537 or 7000A, ΔC and d values are secured and the $\Delta C/d$ ratios computed. On the more precise deflection response range, the bias adjustment is considered satisfactory if values of $\Delta C/d$ do not differ from an average value by more than ±0.5 percent for applied potentials from 0 to 0.3 v. For the maximum useful response range (applied voltage 0 to 0.5 v), the variations of $\Delta C/d$ from a mean value will not exceed ±1.5 percent when the bias is suitably adjusted.

It would be of little value to list the exact bias potentials used on the various sensitivity ranges because there would be some variation for different circuits. However, check experiments with three FP-54 Pliotrons of non-uniform service record and purchase date indicate that the bias potentials and linearity ranges suggested in the curves of Fig. 2 are about the same for all three tubes in the particular circuit used.

In utilizing the deflection method, the exact bias values determined for the circuit should be set on small potentiometers built into the amplifier assembly and switched in as needed. It is also of advantage to provide an Ayrton shunt designed for the linear deflection range. For the particular amplifier and galvanometer system described, the deflections corresponding to 0.3 v and 0.5 v applied grid potentials are, respectively, 975 and 1625 cm, and a shunt having multiplying values 1, 5, 20, and 30 will be used.

TABLE I.

R (OHMS)	$\Delta C/d$ (10^{-16} MHO/CM)	A	LIGHT INTENSITY RESPONSE RANGE (ARBITRARY UNITS)	LIGHT INTENSITY FOR 1-CM RESPONSE (ARBITRARY UNITS)
10^8	3.41	734	0 to 1,000,000	1000
1.08×10^9	0.316	7,932	" " 92,660	92.66
9.3×10^9	0.0367	68,310	" " 10,760	10.76
10^{11}	0.00341	734,000	" " 1000	1

SUMMARY

Typical circuit constants and response data computed for the four linear sensitivity ranges of the spectrophotometer are shown in Table I. At each sensitivity setting, grid bias is adjusted for linear galvanometer response to applied grid potentials from 0 to 0.308 v. As discussed above, in this voltage range deflection is proportional to incident light intensity within ±0.5 percent,

and, by design, the response of the galvanometer system is from 0 to 1000 cm. The arbitrary light intensity unit selected is the relative intensity, at any given wave-length, required to produce a 1-cm galvanometer deflection on the highest sensitivity range ($R=10^{11}$ ohms). On this basis, the instrument can measure, by the deflection method, light intensity values ranging from 1.0 to 10^6 arbitrary units. At the minimum and maximum response levels, approximations of the light flux incident on the photo-cell can be obtained in terms of its sensitivity to tungsten 2870°K radiation. The computed values are, respectively, 2.5×10^{-11} and 2.5×10^{-5} lumen.

A New Photographic Sensitometer

W. M. CADY
Department of Physics, Cornell University, Ithaca, New York

(Received September 15, 1939)

A sensitometer is described which affords a continuous variation of illumination across the sensitive surface. Two intensity-ranges are available, using the same source of light and the same exposure-time; with both ranges, the instrument can give an over-all variation of intensity in the ratio 2000 : 1. No lenses or moving parts are needed, and the sensitometer is strictly neutral with regard to wave-length.

THE sensitometer here described is of the intensity-scale continuous variation type, designated by Jones[1] as I(1). Sensitometers of this type have modulated the intensity of illumination by means of a sector disk rotating enough times during the exposure to avoid the intermittency effect,[2] or by a neutral absorbing screen of non-uniform density, or by cylindrical lenses.[3] The present instrument, though reminiscent of those described by Kinder, contains the advantages of simplicity and wide intensity-range.

The arrangements described by Kinder all use one or more large cylindrical lenses and an opaque screen with an aperture of which the form determines the variation of intensity. Each of these arrangements is open to the objection that the ratio of extreme intensities is equal to the ratio of the maximum to minimum width of the wedge-shaped aperture; and the latter ratio cannot well greatly exceed 100 : 1 if the aperture is to be reasonably small and accurately constructed to some desired form.

The present device produces a logarithmically varying illumination with a range of about 50 : 1 on a three-inch strip of emulsion, and after a simple change affords another but weaker illumination on another strip of emulsion, which also varies logarithmically and with the same 50 : 1 ratio. The two intensity ranges overlap somewhat, to give an over-all variation of some 2000 : 1.

The essential parts of the present sensitometer are shown in Fig. 1. A lamp L is installed in a ventilated housing at a fixed distance (which need not be known) from a sheet A of opal glass, which forms one end of a rectangular wooden box $ABCDE$ of inside dimensions $5\times6\times33$ in. Between A and another sheet B of opal glass, the box is internally coated with aluminum paint to improve the uniformity of illumination of B. The remainder of the box is blackened and provided with light-baffles. In contact with the right-hand face of B is a brass screen C; the peculiar perforation in C is described below. In the plane D there may be installed either of two screens: one, used in making the high intensity exposure, is simply a vertical straight-edge which covers, from the point of view of C, the right-hand half of the cross section of the box, while the alternative screen, used in making the low intensity exposure, is a long vertical slit about 0.017 in. wide and centrally located. A plateholder at E holds the photographic material.

The aperture in the screen C is pictured in Fig. 2. The curve is, for $0\leqslant\xi\leqslant3$ in., $\eta=3\times10^{-k\xi}$ in., and the area to the right of $\xi=3$ in. is equal to the area which would underlie this curve if extended from $\xi=3$ in. to infinity, i.e., equal to

$$\int_3^\infty 3\times10^{-k\xi}d\xi \text{ sq. in.}$$

In the present instrument, $k=0.571$ in.$^{-1}$.

If at D the straight-edge is installed, then the various parts of the emulsion can "see" various

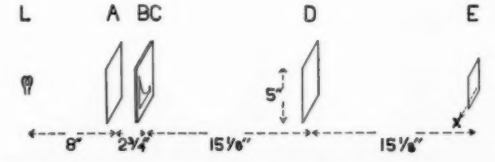

FIG. 1. Schematic perspective view of the sensitometer.

[1] L. A. Jones, *Photographic Sensitometry* (Eastman Kodak Company, 1934).
[2] L. Silberstein and J. H. Webb, Phil. Mag. **18**, 1 (1934).
[3] W. Kinder, Zeits. f. Instrument. **56**, 393 (1936).

proportions of the aperture; indeed the illumination of the emulsion follows an exponential law, with the value of k quoted above. With the slit instead of the straight-edge at D, the illumination again varies with x (Fig. 1) according to the same law (even if the slit-width is not small) but is everywhere weaker than with the straight-edge by a factor depending upon the width of the slit. This width determines the extent to which the two intensity ranges overlap.

In practice the two sensitometric strips are exposed on the same sample of photographic material, the plateholder being lowered after the first exposure. Figs. 3a and 3b show the sort of density curves obtained by using the slit and the straight-edge, respectively. These two curves are fitted together as in Fig. 3c. The contrast γ of the emulsion can be found from this curve, since its slope can be measured and k is known.

For a determination of the speed of the emulsion, it is necessary to know the illumination in some absolute units at any one point of the characteristic curve of Fig. 3c. The illumination at t is indeed known, for this point receives light from the entire rectangular "tail" of the aperture; and the candlepower of this tail can be determined by dividing the measured candlepower of the entire aperture by the known ratio of areas of the tail and the aperture.

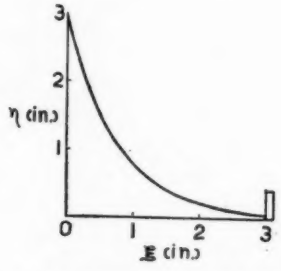

FIG. 2. The aperture shown at C, Fig. 1.

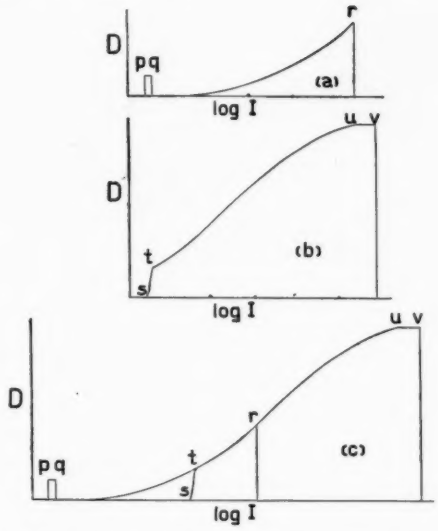

FIG. 3. A characteristic curve (c), showing the relationship between the density D and the intensity I, and formed by combining the two partial curves (a) and (b). Here (a) was exposed through the slit, the region pq being a sort of pinhole image of the rectangular part of the aperture of Fig. 2. Varying amounts of this rectangle are effective between s and t in (b), which was exposed with the straight-edge. The region uv can "see" the entire aperture. The useful part of the curve (c) is qu.

The speed of this sensitometer is such that a fast emulsion would require 0.1 or 0.2 sec. of exposure if the illumination is provided by a 115-v, 400-w gas-filled tungsten lamp operated at 105 v. A weaker lamp would make the exposures conveniently long, but reciprocity error would result if the material is to be used with short exposures.

Error in the illumination of the emulsion may arise from several sources, the most important being the variation of the brightness of the opal glass B (± 1 percent), and the failure of the curved aperture to follow the exponential formula (± 1.2 percent).

Theory of the Double Fizeau Toothed Wheel

HERBERT E. IVES
Bell Telephone Laboratories, New York, New York
(Received July 13, 1939)

I

IN a discussion of the theory of relativity, R. W. Wood[1] has considered a modification of Fizeau's method for determining the velocity of light, in which two toothed wheels are mounted at the ends of a long axle, and light is sent in one direction only. If such an apparatus, rotated while stationary at such a speed that light passing through a tooth in the near wheel is transmitted by a given tooth in the distant wheel, is then set in motion in the direction of the axis of rotation, the velocity of light relative to the apparatus will be changed so that transmission will no longer take place, unless some alteration in dimensions or shape occurs. A Fitzgerald contraction of length, by the factor $(1-v^2/c^2)^{\frac{1}{2}}$, where v is the translational velocity, will not restore transmission, since the changed velocity of light is $c\pm v$. Wood concludes that there must be an additional compensating factor, namely a twist of the axle. F. E. Hackett[2] has discussed the same problem more in detail, and considers the "twist" as analogous to the twist of a steel tube placed in a coaxial spiral magnetic field (Wiedemann effect).

It is the purpose of this paper to point out that this "twist" is not a phenomenon peculiar to rotation, or supplementary to the Fitzgerald contraction; it is a necessary result of that contraction when any uniformly moving body is constrained to a definite orientation. The Fitzgerald contraction (in conjunction with the Larmor-Lorentz change of rate of a clock in motion) suffices in fact to elucidate all problems connected with the behavior of rotating disks set in uniform translational motion.

Consider the double Fizeau toothed wheel of Wood, which is shown schematically in plan view in Fig. 1. Here W_1 and W_2 are the two toothed wheels, mounted on the axle A. The tops of the wheels, which are presented to the observer, are in motion toward the right, with the velocity $V=r\omega$. The apparatus as a whole is moving with the velocity v in the direction parallel to the axle. We have at once that a rectangular element of the cylinder bounding the wheels, a_1, a_1', b_1, b_1', is moving at the instant depicted, with the velocity $R=(v^2+V^2)^{\frac{1}{2}}$ in a direction inclined to the axle by the angle $\theta=\tan^{-1} V/v$. The immediate problem is to determine the shape taken by the elementary rectangle a_1, a_1', b_1, b_1', due to the Fitzgerald contraction.

This problem may be profitably studied in two steps. As the first step we consider the element a_1, a_1', b_1, b_1', as a rectangle symmetrically disposed about a line xx', at right angles to the direction of motion and maintaining its orientation unchanged when in motion (Fig. 2). For purposes of clear exposition let us take the components of velocity large as compared with the velocity of light, e.g. $v=0.8$ c, $V=0.4$ c. The resultant shape of the elementary rectangle is obtained by reducing the normal distances of all points from the line xx' in the ratio $(1-R^2/c^2)^{\frac{1}{2}}:1$. This gives us the figure, a_2, a_2', b_2, b_2'; the rectangle becomes a rhomboid whose sides are inclined both to the axle and to the planes of the wheels.

This shape cannot represent the true condition in the toothed wheel system of Fig. 1, since the horizontal sides of the element are actually mechanically constrained to be perpendicular to

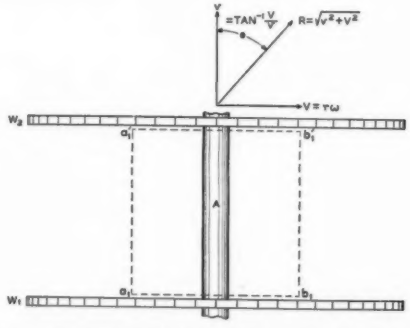

FIG. 1. Plan view of double Fizeau toothed wheel.

[1] R. W. Wood, *Physical Optics* (Macmillan, second edition, 1911), p 690.
[2] F. E. Hackett, Phil. Mag. **44**, 740 (1922).

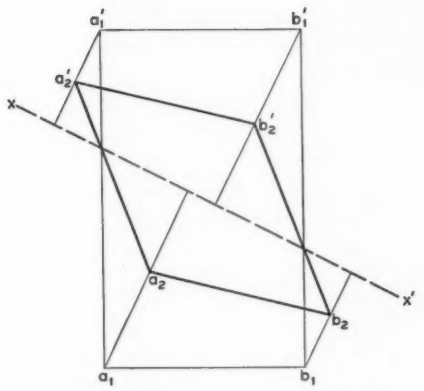

FIG. 2. Fitzgerald contraction of rectangle.

the axle. We must therefore find the contracted shape conforming to this condition. To do this we follow the construction shown in Fig. 3. We have as before the axis xx', normal to the direction of motion and contraction, which we select as passing through a corner b_1, of the rectangle. We take any point p' on the toothed wheel W_1 whose perpendicular distance from xx' is s', and note that before contraction its perpendicular distance from xx', which we will call s, must be $s'/(1-R^2/c^2)^{\frac{1}{2}}$. This gives us the point p, which is a point on the side of the rectangle which, in motion, because of the contraction, will be on W_1. We now proceed to erect on the line determined by the fixed corner of the rectangle b_1 and p, an undistorted, uncontracted rectangle, similar to a_1, a_1', b_1, b_1', which we may identify by the same letters with the subscript 2, namely a_2, a_2', (b_1), b_2'. We next subject this rectangle to the contraction $(1-R^2/c^2)^{\frac{1}{2}}$, normal to xx', by the same procedure as before, giving us finally the rhomboid, a_3, a_3', b_1, b_3', a figure which has the shape and the orientation assumed by our original rectangle under the Fitzgerald contraction when mechanically constrained to have its base coincide with W_1.

It is now necessary to show that the rhomboid a_3, a_3', b_1, b_3', owing its shape solely to the Fitzgerald contraction under mechanical constraint, possesses the exact shape and dimensions to insure invariance in the behavior of the double Fizeau toothed wheel,—in other words that its shape is equivalent to a Fitzgerald contraction in the direction of motion of the system of value $(1-v^2/c^2)^{\frac{1}{2}}$, plus a "twist" of the right value.

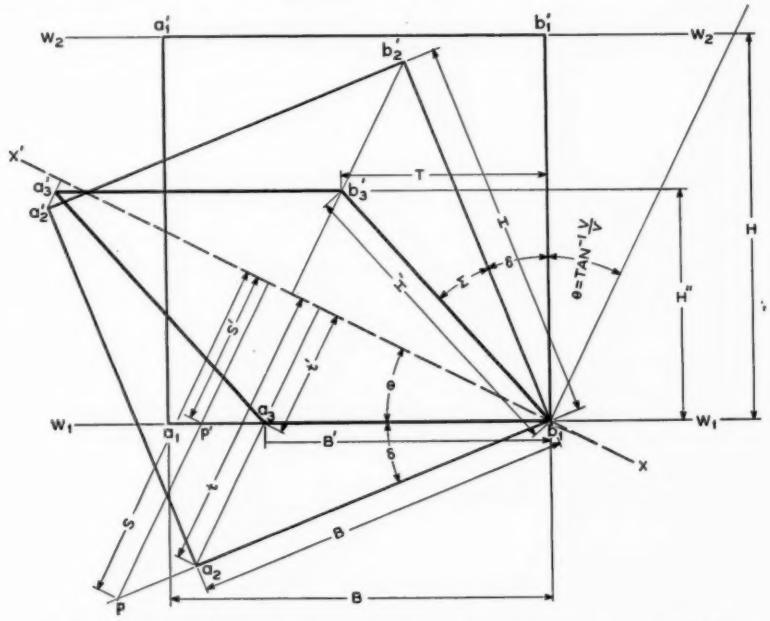

FIG. 3. Construction for determining Fitzgerald contraction of rectangle with base constrained to definite orientation.

In order to carry through this proof we first apply distinguishing designations to the various distances and angles in Fig. 3, as follows:
the base of the original rectangle, $a_1-b_1=B$,
the altitude of the original rectangle, $a_1-a_1'=b_1-b_1'=H$,
the base of the final rhomboid, $a_3-b_1=B'$,
the side of the final rhomboid, $b_3-b_1=H'$,
the altitude of the final rhomboid $=H''$,
the displacement of b_3' from the original side, $b_1-b_1'=T$,
the angle between the tilted rectangle, a_2, a_2', b_1, b_2' and $W_1=\delta$,
the angle between b_1-b_3' and $b_1-b_1'=\delta+\epsilon$,
the uncontracted normal distance of a_2 from $xx'=t$,
the contracted normal distance of a_2 from $xx'=t(1-R^2/c^2)^{\frac{1}{2}}=t'$.

Proceeding now first to the determination of B' we have, from the oblique triangle a_2, a_3, b_1

$$B'=B\frac{\cos(\theta+\delta)}{\cos\theta} \tag{1}$$

and

$$\frac{\tan(\theta+\delta)}{\tan\theta}=\frac{t}{t'}=\frac{1}{(1-R^2/c^2)^{\frac{1}{2}}}. \tag{2}$$

From (2) we get by elementary trigonometric transformations, the value of $\cos(\theta+\delta)$, giving finally

$$B'=B\frac{(1-R^2/c^2)^{\frac{1}{2}}}{\cos\theta(1-(R^2/c^2)+\tan^2\theta)^{\frac{1}{2}}}. \tag{3}$$

By a series of similar operations, involving intricate but straightforward transformations, which need not be repeated here, we obtain

$$H'=H\left(\frac{\tan^2\theta+(1-R^2/c^2)^2}{\tan^2\theta+(1-R^2/c^2)}\right)^{\frac{1}{2}}, \tag{4}$$

$$H''=H\left(\frac{\tan^2\theta+(1-R^2/c^2)^2}{\tan^2\theta+(1-R^2/c^2)}\right)^{\frac{1}{2}} \cdot\frac{\tan^2\theta+(1-R^2/c^2)}{([\tan^2\theta+(1-R^2/c^2)]^2+R^4/c^4\tan^2\theta)^{\frac{1}{2}}}, \tag{5}$$

$$T=H\left(\frac{\tan^2\theta+(1-R^2/c^2)^2}{\tan^2\theta+(1-R^2/c^2)}\right)^{\frac{1}{2}} \cdot\frac{(R^2/c^2)\tan^2\theta}{([\tan^2\theta+(1-R^2/c^2)]^2+R^4/c^4\tan^2\theta)^{\frac{1}{2}}}. \tag{6}$$

These formulae, upon substituting $\tan\theta=V/v$, and $R^2/c^2=V^2/c^2+v^2/c^2$ and arranging terms, take the simple forms:

$$B'=B\left(1-\frac{V^2}{c^2(1-v^2/c^2)}\right)^{\frac{1}{2}}, \tag{7}$$

$$H'=H\left(1-\frac{v^2}{c^2}+\frac{V^2v^2}{c^4(1-v^2/c^2)}\right)^{\frac{1}{2}}, \tag{8}$$

$$H''=H(1-v^2/c^2)^{\frac{1}{2}}, \tag{9}$$

$$T=H\frac{Vv}{c^2(1-v^2/c^2)^{\frac{1}{2}}}. \tag{10}$$

We are now ready to compare the behavior of the double-toothed wheel system when stationary, and when moving in the direction of its axle with the velocity v.

Taking first the stationary case, we have on putting V_s for the peripheral velocity of the disks, the simple relation

$$V_s/c=d/H, \tag{11}$$

where d is the distance from the leading side of the rectangle that a light beam from b_1, projected normally to W_1, will hit. Substituting $r\omega$ for V_s we get

$$d=Hr\omega/c. \tag{12}$$

For the double Fizeau-disk system in motion we have the following relations

$$H''+vt=ct, \tag{13}$$

$$d'=V_mt-T, \tag{14}$$

where V_m is the peripheral velocity with the system moving; and t is the time required for the light signal to traverse the moving rectangle; from which,

$$d'=VH''/(c-v)-T. \tag{15}$$

Using (9) and (10) this gives

$$d'=\frac{HV_m}{c(1-v^2/c^2)^{\frac{1}{2}}}. \tag{16}$$

We now consider the significance of the terms $V/(1-v^2/c^2)^{\frac{1}{2}}$ in (7), (8), (9) and (10). Remembering that when the system is set in motion with the velocity v the clock by which we measure the angular velocity of the disk goes slower in

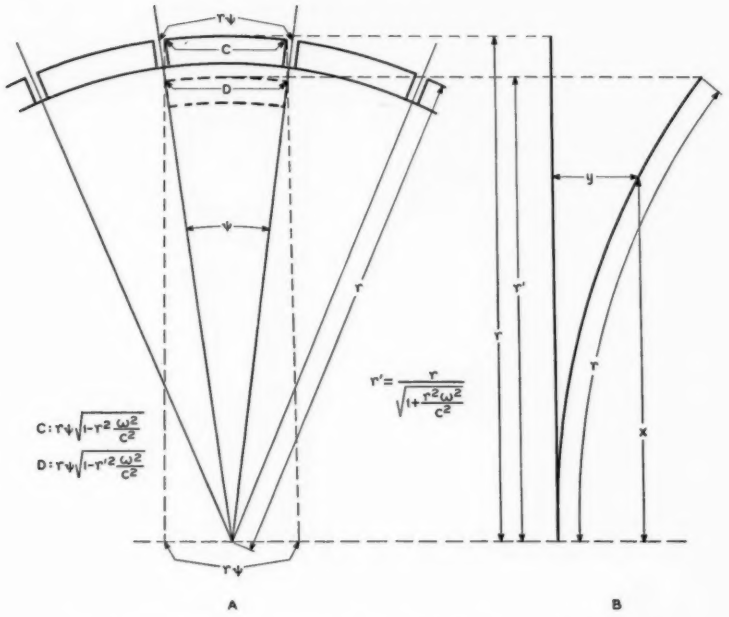

FIG. 4. "Dishing" of a rotating disk subject to Fitzgerald contraction.

the ratio $(1-v^2/c^2)^{\frac{1}{2}}$, we see at once that $V_m = V_s(1-v^2/c^2)^{\frac{1}{2}}$ when the angular velocity is set at the same apparent value. Hence (16) becomes:

$$d' = HV_s/c = Hr\omega/c, \tag{17}$$

so that by comparison with (12)

$$d' = d. \tag{18}$$

We find therefore that the Fitzgerald contraction is of itself sufficient to give both the contraction in the direction of motion (9) and the "twist" (10) necessary to insure the invariance of behavior of the apparatus when in motion at right angles to the plane of the toothed wheels.

II

The above solution of the Fizeau double-toothed wheel problem in terms of Fitzgerald contraction alone prompts the discussion along similar lines of some associated problems in the behavior of rotating disks, which are considered in this and the succeeding sections.

From the above discussion it follows that the two toothed wheels suffer a contraction of peripheral length. This contraction must occur for each wheel, and, by placing $v=0$, we see that for a single stationary rotating disk the periphery must be contracted in the ratio $(1-r^2\omega^2/c^2)^{\frac{1}{2}} : 1$. A difficulty here arises, pointed out by Ehrenfest, that a radius of the disk, which is moving transversely to its length, will suffer no contraction, thus conflicting with the elementary relation between the diameter and the periphery of a circle. This problem has been considered by Lorentz, and by Eddington,[3] who decide by methods involving the general theory of relativity, that both periphery and radius must contract alike, by the factor $(1-\frac{1}{4}v^2/c^2)^{\frac{1}{2}}$. This solution appears incompatible with the results of Section I.

A solution in terms of the simple Fitzgerald contraction is possible if we abandon a condition which is usually tacitly assumed in the Ehrenfest paradox, namely that the disk must remain *flat*. The nature of this solution is at once evident on

[3] A. S. Eddington, *Mathematical Theory of Relativity* (Cambridge University Press, 1923), p. 112.

recalling the shape which is given to a circular saw blade in order that, when in rotation, it shall resist the outward stresses set up by the high peripheral velocity. The saw blade is made in a "dished" shape, and becomes flat at high speeds. We have with the Fitzgerald contraction an inverse condition, the disk is under stress to become smaller instead of larger. The solution is for it to be flat when not rotating, to "dish" as it rotates.

We may calculate the configuration of the rotating disk by the construction shown in Fig. 4, where a section of the disk is shown in plan at A, in profile at B. Referring to A, a peripheral element of the disk of length $r\psi$ assumes, because of the Fitzgerald contraction, the length $r\psi(1-r^2\omega^2/c^2)^{\frac{1}{2}}$. By so doing it becomes shorter than the section of the (uncontracted) periphery which it occupied when stationary. In order to bring all the so shortened peripheral elements into contact again, each element must be moved toward the center. In being so moved however an element increases in length (by decreasing its Fitzgerald contraction) due to the decreased velocity as the radial distance becomes smaller. Denoting the radius at which the moved element just touches the next as r', we express the relationship resulting as follows:

$$r'\psi = r\psi\left(1-\frac{r^2\omega^2}{c^2}\right)^{\frac{1}{2}}\left[\frac{(1-r'^2\omega^2/c^2)^{\frac{1}{2}}}{(1-r^2\omega^2/c^2)^{\frac{1}{2}}}\right]$$

or

$$r' = r(1-r'^2\omega^2/c^2)^{\frac{1}{2}}, \tag{19}$$

from which

$$r' = \frac{r}{(1+r^2\omega^2/c^2)^{\frac{1}{2}}}. \tag{20}$$

Remembering that the length of the radius r is unaffected by the rotation, we see from B that the prescribed configuration of the radius is a curve of length r for which the relationship (20) is obeyed. This is shown in Fig. 4B.

In order to determine the equation of this curve, let y be the distance of any point on the curve from the stationary trace, and $x(=r')$ the distance of the point from the axis. Calling $\omega^2/c^2=\alpha^2$,

$$r = \frac{x}{(1-x^2\alpha^2)^{\frac{1}{2}}},$$

$$dr = \frac{dx}{(1-\alpha^2x^2)^{\frac{1}{2}}},$$

$$\left(1+\left(\frac{dy}{dx}\right)^2\right)^{\frac{1}{2}} = \frac{dr}{dx} = \frac{1}{(1-\alpha^2x^2)^{\frac{1}{2}}},$$

$$\left(\frac{dy}{dx}\right)^2 = \frac{1}{(1-\alpha^2x^2)^3} - 1,$$

$$dy = \frac{\alpha x(3-3\alpha^2x^2+\alpha^4x^4)^{\frac{1}{2}}}{(1-\alpha^2x^2)^{\frac{1}{2}}}dx,$$

the integral of which is

$$y = \frac{\sqrt{3}}{2} - \frac{((3+\alpha x^2)(1-\alpha x))^{\frac{1}{2}}}{2} + 2\left[\tan^{-1}\left(\frac{1-\alpha x^2}{3+\alpha x^2}\right)^{\frac{1}{2}} - \tan^{-1}\frac{1}{\sqrt{3}}\right]. \tag{21}$$

When ω is small

$$dy/dx \cong \sqrt{3}\alpha x,$$

$$y \cong \frac{\sqrt{3}}{2}\alpha x^2 = \sqrt{3}\frac{r'^2\omega}{c}, \tag{22}$$

or the disk assumes an approximately paraboidal shape.

The contraction in diameter, and the dishing, produced by the Fitzgerald contraction, are measures of *rotation with respect to the ether*—not of *relative* rotation of material bodies. Two similar disks in relative rotation cannot each be contracted in diameter with respect to the other. It follows that by rotating a disk at such a speed that it exhibits maximum diameter we establish that it has no rotational motion with respect to the ether.

III

In the problem of the double Fizeau toothed wheel as treated in Section I the effect of the translational motion of the system is relatively simple, since the axial symmetry of the disks is unaffected by motion at right angles to their

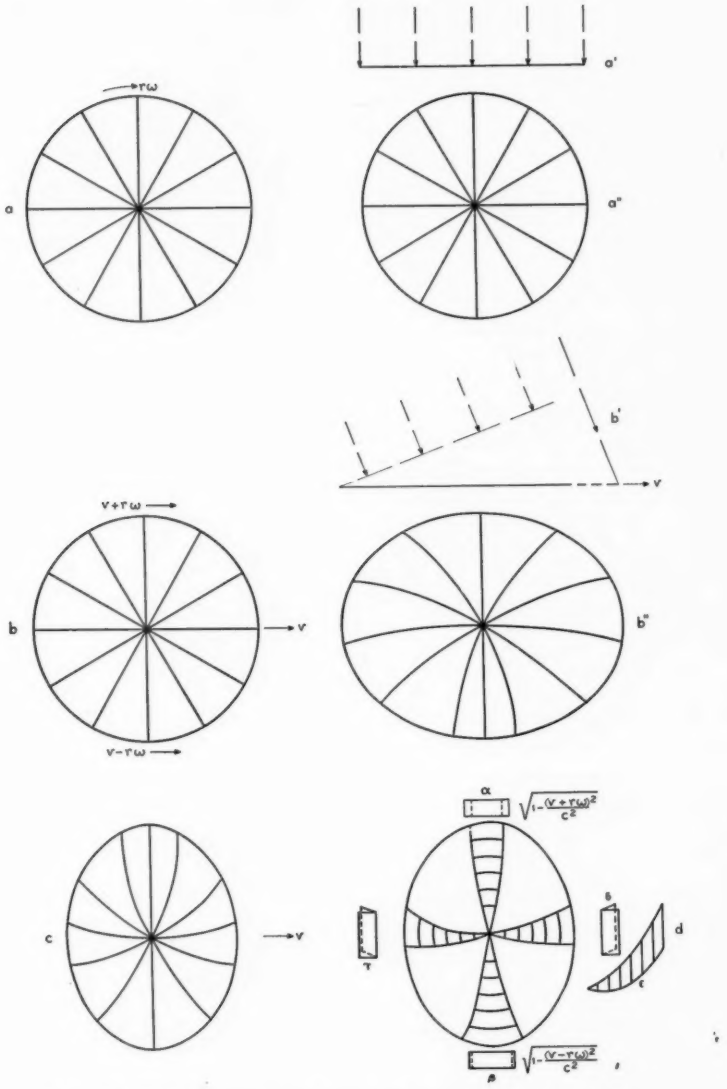

FIG. 5. Fitzgerald contraction of rotating disk moving in its own plane.

planes. A more complicated problem is presented when the translational motion is at some other angle to the plane of a rotating disk, for instance parallel to that plane. In this case, (Fig. 5b) the velocities of elements of the periphery range from $v+r\omega$ to $v-r\omega$, calling for different Fitzgerald contractions at different points.

I shall not present a detailed treatment of this case, but will confine myself to showing that the Fitzgerald contractions are of the required character to produce a configuration of the disk which will mask the effects of the translational motion. I shall attack this problem in the reverse direction from that followed in Section I, taking up first the results to be expected from optical observation without the occurrence of any form of contraction, deduce from these what the contractions need to be to offset the optical effects

introduced by motion, and compare these with the contractions as predicted by the analysis used above in connection with Fig. 3.

Assume a flat opaque disk (Fig. 5a) rotating with the angular velocity ω. Suppose it to be perforated with a number of radial slits. Now let a light flash be originated from a distant point on the upwardly produced axis (Fig. 5a′) and, passing through the disk, fall upon a light sensitive surface, such as a photographic plate. The trace so obtained will be (Fig. 5a″) an exact copy of the disk.

Let us next set the disk in motion to the right (Fig. 5b) with the velocity v. Owing to the motion the light flash from the distant point on the axis no longer meets the disk normally, but at the angle $\sin^{-1} v/c$; (Fig. 5b′) the leading edge of the disk is recorded later than the following edge, it will have traveled a distance greater than the diameter, and the radial slits will, during this interval, have turned about the axis. As a result the photographic trace of the disk will be a lengthened ellipse; the traces of the slits will be curved lines, as shown in Fig. 5b″.

If the rotating disk in motion is to yield an optical record which shall be indistinguishable from the record of the stationary disk (which is, broadly speaking, what the Fitzgerald contraction was invented to do) the disk must assume a configuration of a character inverse to b″. It must be contracted in the direction of motion; its slits must have the opposite curvature to those of the trace b″. The necessary disk configuration is that shown in Fig. 5c.

It now remains to show that the distorted disk 5c with its curved slits is the figure that the original circular disk with radial slits would assume as a result of the Fitzgerald contraction. Referring to Fig. 5d we see how this can come about. At α and β are shown peripheral elements of the circular disk moving parallel to the direction of translation, as they would be contracted due to their velocities, α showing greater contraction than β because of its greater velocity ($v+r\omega$ as against $v-r\omega$). At γ and δ are shown peripheral elements moving transverse to the direction of translation. These, constrained on their sides toward the center of the disk, are warped, according to the analysis of Section I into rhombs, whose transverse diameter is reduced by the factor $(1-v^2/c^2)^{\frac{1}{2}}$. Finally consider, at ϵ, the configuration taken by a series of radial elements starting at the center of the disk. These will be increasingly warped with increasing radial distance, and being constrained to remain in contact, will take the horn-shape shown. It is clear, without more detailed analysis, that the configuration c is that produced by the Fitzgerald contraction.[4]

[4] Both stationary and moving rotating disks are subject also to the dishing effect already discussed.

Apparatus for a Long Optical Path in a Restricted Space

F. T. ROGERS, JR.*
The Rice Institute, Houston, Texas
(Received September 5, 1939)

MANY ingenious and satisfactory devices have been described for obtaining in a restricted region a long optical path. For example, Badger, Bonner, and Cross[1] have described their use of $\frac{7}{8}$-in. I. D. stainless steel tubing, highly polished inside, to construct a 70-foot long absorption tube. This tube would serve in place of the usual optical system to confine the light in the desired path. In the following paragraphs is an account of the design and construction details of an apparatus of an entirely different nature, which can produce the same path length (in approximately the same volume of gas) in a much shorter length of tube.

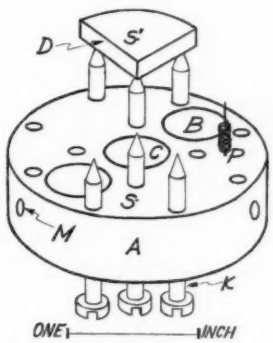

FIG. 1.

A bank of mirrors like that shown in Fig. 1 was placed in each end of a 14-foot length of 2-in. iron pipe to obtain (for infra-red absorption work) an optical path length of 36 meters. Each bank consists of four small, individually adjustable, front-surfaced plane mirrors; the shop work on one can be done very easily and quickly.

Figure 1 shows in adequate detail a bank in partial assembly. Parts A and D are of blackened brass; P are piano-wire springs, soft-soldered into the small holes at S and S'. K are standard 8–36 iron bolts, sharpened on their ends; their ends fit into suitably located small drill-tip depressions in the parts D. M are drill-tip depressions (spaced 120° apart) made with a $\frac{3}{8}$-in. drill; they are used for mounting the mirrors in the 2-in pipe. B and C are $\frac{1}{2}$-in. holes. The small mirrors are spotted to the D's with rosin-and-beeswax.

In use, holes C are for light to enter and leave the 2-in. pipe. Holes B are for telescopic observations of the mirror-aligning process.

To determine an optical system which has a narrow enough beam of light to stay entirely on the mirrors, let h = the greatest diameter of the light source, H = the smallest diameter of the mirrors, L = the total length of the light path from the condensing lens (outside the 2-in. pipe at the entering end) to the detector (such as spectrograph slit) of radiation which has passed through the absorption tube, d = distance from the condensing lens to the light-source, a = the diameter of the condensing lens, and f = the focal length of the condensing lens. Then simply choose d, a, and f such that

$$d \leqq hL/H, \tag{1}$$

$$a \geqq H, \tag{2}$$

$$f \leqq hL/(h+H). \tag{3}$$

These equations are valid only if all windows, which allow light to enter and leave the mirror and pipe system, have diameters $\geqslant H$.

* Now at The Yerkes Observatory, Williams Bay, Wisconsin.
[1] R. M. Badger, L. G. Bonner, and P. C. Cross, J. Opt. Soc. Am. **25**, 355 (1935).

A New Method for Testing Cassegrain Mirrors

E. GAVIOLA
Observatorio Nacional, Córdoba, Argentina
(Received August 31, 1939)

A new arrangement for testing Cassegrain mirrors is described which does not require the use of large mirrors as auxiliaries. It consists in placing a convergent lens in front of the mirror so as to form a real image of the illuminating pinhole and measuring the resulting aberration. The aberration of the lens is numerically eliminated after an independent measurement with the help of a small plane mirror placed at an appropiate distance. The longitudinal aberration of the Cassegrain alone can also be directly obtained by displacing the small plane mirror. The method permits high precision. It can be applied to any convex surface.

THE problem of testing accurately a Cassegrain reflecting telescope mirror has been up to now a difficult one. The autocollimation method of Ritchey requires the use of the main parabolic mirror of the telescope, of a master flat of at least the same size and of a spherical mirror of as large a diameter to test the flat. The central part and the peripheral zone of the Cassegrain—needed for having a finite field—cannot be seen nor tested. One has to use light that has suffered five—if the parabolic mirror is not perforated, seven—reflections, so reducing the accuracy of the test. It is thus practically impossible to test the Cassegrain with precision (equal to or higher than that of) the parabolic, as would be desirable.

Hindle eliminates several of these drawbacks by using instead of the flat + parabolic combination, a spherical mirror of a size about the same as the parabolic and of about half its radius of curvature. The unseen zone in the center is now reduced to a minimum and the rest is visible to the very edge. As the spherical mirror can easily be tested and therefore made with great accuracy, the survey of the Cassegrain can be made nearly as accurate. The difficulty involved in the use of Hindle's method is the need of a large spherical mirror that generally has to be made specially for the purpose. For large telescopes this procedure becomes prohibitive.

Most observatories possessing telescopes with Cassegrains do not have large plane or spherical mirrors and have no optical shops that could build them. The resource of testing the Cassegrain from the back through the glass is unsatisfactory as there is no way of controlling independently the errors introduced by the irregularities of the glass. The test of the Cassegrain in the telescope with starlight can never be accurate as there is no possible temperature control. Besides, the center and the peripheral zone cannot be seen from the axis. The use of a complementary spherical or hyperbolic concave mirror to produce interference fringes upon superposition, offers large practical difficulties. Its accuracy cannot be carried very far.

In 1936, while at the La Plata Observatory, I was confronted with the problem of testing and correcting the Cassegrain mirror of its 82-cm reflector. It was apparent that it had errors exceeding half a wave-length. As we had no plane mirror of that size and no possiblity of making either a flat or a Hindle spherical of 82-cm diameter it became necessary to find a new simple method for testing the Cassegrain using only the available equipment. After some experiments a satisfactory method was devised.

PRINCIPLE OF THE METHOD

The new method is based on the following considerations:

In order to test an optical surface we need an arrangement that will form an image of some kind. If the image is very good the study of it is generally sufficient to tell about the quality of the optical surface or system. This is the qualitative null or autocollimation method. If the image is not so good we subdivide it into a number of good images by decomposing the main optical surface into sufficiently small parts or zones. One can always calculate the aberrations of the system or the curve of shape of the surface by *measuring the relative positions* of the partial images, observing one after the other. This

method is quantitative and—if properly applied—more exact than the former one.

If the image is not formed by the optical surface to be tested alone but with the help of an auxiliary optical system, it is necessary to have an independent test for the auxiliary system.

To make a convex reflecting surface form an image of some kind of "artificial star" or slit one can, among other things, put a convergent lens in front of it. The lens has to have a focal distance smaller than the radius of curvature of the convex surface. Its diameter has to be only slightly larger. These are the two necessary conditions. The lens may be simple or compound. It may have any amount of errors. Its chromatic aberration is eliminated by using monochromatic light.

The independent test of the auxiliary system is accomplished by removing the Cassegrain and placing a small plane mirror at an appropriate distance. Once this is done, the aberrations of the lens are numerically excluded.

Description of the Method

Let C be the Cassegrain mirror to be tested, L the auxiliary lens and S a zonal screen put between the two (Fig. 1a). Using a Foucault knife-edge apparatus in which parallax has been eliminated[1] so that knife-edge and slit are always virtually coincident and applying monochromatic light to the slit, we determine the position of the image O formed by the central zone of the screen along the optical axis $O-O'$. Taking O as the nullpoint of the scale we measure the distances y' of the mean positions of the images—centers of least confusion—formed by every pair of zones of the screen. These values y' will be called the longitudinal aberrations of the optical system lens+Cassegrain. We now remove the Cassegrain, leaving knife-edge, lens and screen untouched, and place a small plane mirror M at a distance F_1 from the lens (Fig. 1b) in such a way that, the slit and knife-edge being at O, the image of the slit formed by the central zone of the screen falls again on O. Leaving M in this position we measure the longitudinal aberrations y of the lens for each pair of zones. If the Cassegrain were spherical we would obtain the same values as before. As it is not we find that the differences $y'-y$ are not zero. These differences measure the longitudinal aberrations of the Cassegrain alone. In order to calculate its curve of shape we have to compare them with the theoretical aberrations. If the convex surface of the Cassegrain could be observed from behind without the disturbing influence of the glass it would appear as what the mirror makers call an overcorrected paraboloid. The longitudinal aberrations of the theoretical surface—a hyperboloid

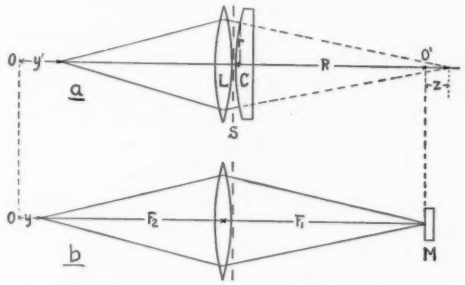

FIG. 1. Experimental arrangement for testing a Cassegrain mirror. Above: determination of the longitudinal aberration of the system Cassegrain + lens. Below: Longitudinal aberration of the lens alone.

of radius R and eccentricity e—would be given by

$$Z_t = e^2 r^2/2R, \tag{1}$$

where r is the mean radius of each screen zone projected on the Cassegrain. The radius of curvature R of the central zone is found by measuring the distance between the surface of the small plane mirror M and the convex face of the Cassegrain.

In order to compare $(y'-y)$ with Z_t we have to bring both to the same side of the lens. This is easily done if we remember that

$$\Delta F_1 = -(F_1/F_2)^2 \Delta F_2. \tag{2}$$

If we call Z_m the measured aberration of the Cassegrain transported to the other side of the lens, we have then

$$-Z_m = (F_1/F_2)^2 (y'-y). \tag{3}$$

These are the values to be compared with the theoretical aberration (1).

If we want to obtain the curve of shape of the mirror we use the well-known formula

$$-\Sigma h = \Sigma z r d R^{-2}, \tag{4}$$

[1] E. Gaviola, J. Opt. Soc. Am. **26**, 166 (1936).

where h is the increment in height across a zone of width d and mean radius r.

If for Z we use the measured values Z_m we obtain the curve of shape referred to the sphere. If we put $Z=Z_m-Z_t$ we obtain the resultant curve of shape referred to a theoretical hyperboloid. One can change the radius of curvature of the hyperboloid of reference simply by adding a constant, but otherwise arbitrary, amount to Z_m.

Discussion and Refinements

While applying formulas (2) or (3) one has to remember that F_1 is constant for all the zones of the screen; but not so F_2, which varies from zone to zone. If the lens L is corrected for spherical aberration for the monochromatic light used and for the image distance F_1, then F_2 and the conversion factor $(F_1/F_2)^2$ are constant. Otherwise they are not, and one has to set for F_2 the value corresponding to each particular zone. When the spherical aberration is not too large, a mean value can be used for F_2.

For high precision measurements a further point has to be considered. If the convex mirror C is not spherical, the light beam reflected by it and passing a certain hole in the screen does not go exactly through the same part of the lens as when the plane M is used for that particular zone. If, furthermore, the lens has bad secondary zones, a small deviation of the light beam could affect the accuracy of the determined longitudinal aberrations y of the auxiliary system because the factor $(F_1/F_2)^2$ could not be considered constant even for the neighborhood of a single zone. This may be the case if the glass of the lens is of very poor quality. But even in this case the method can be applied with any desired accuracy. All that is necessary is to measure directly the aberrations Z of the Cassegrain by displacing the small plane mirror M with a micrometer screw parallel to the optical axis of the system.

An Alternative Method of Measuring

Once we have determined the values y' of the longitudinal aberration of the Cassegrain+lens system for each zone of the screen as described above, we remove the Cassegrain without changing the relative positions of lens, screen and knife-edge and place the small plane mirror M on a table that can be moved parallel to the optical axis by means of a micrometer screw and divided drum. After adjusting the mirror M properly we measure its axial displacements necessary to reproduce the readings y' on the knife-edge side of the lens for each zone pair of the screen. These displacements, counted from the position corresponding to the central zone, measure directly the longitudinal aberration Z_m of the Cassegrain. No correction or calculation is now necessary. The light now traverses exactly the same part of the lens in the two cases. The lens may be therefore as bad as the worst without affecting the accuracy of the measurement. It is not necessary to know the values F_1 and F_2. The radius of curvature of the central zone of the Cassegrain is found as before. The displacements Z_m of the mirror M can now be directly compared with the theoretical values Z_t given by Eq. (1). The integration is done as before.

In actual practice it is seldom necessary to reproduce the readings y' exactly. One can place the mirror M in a certain number of positions, read the new values of y' and obtain afterwards the exact value Z_m by interpolation. The exact determination of the nullpoint of the Z_m scale is not important, as one can add an arbitrary constant amount to the quantities in order to choose the most appropriate hyperboloid of reference.

Instead of the plane mirror M a concave spherical can be used, placing it at the distance R plus its own radius of curvature from the convex surface of the Cassegrain.

The Main Source of Errors

While applying this method to the Cassegrain of the La Plata reflector, with the crown part of an old lens and a small spherical mirror or short radius of curvature as auxiliary system, it was soon apparent that the main source of errors lies in the difficulty of measuring y' or y with sufficient accuracy when $\Delta y/\Delta r$ has values above a certain limit. This difficulty is not confined to the method here described. It is encountered also when testing a parabolic mirror of large relative aperture at the so-called "center of curvature," and in general whenever the longitudinal aber-

ration of the optical system changes rapidly with the radius of the circular zone. The difficulty consists in the following. While cutting the light of a symmetrical pair of zones near the periphery, with the knife-edge, in the usual way, it is observed that a photometric comparison of the reduction of the intensities of the two opposite parts of the zone becomes impossible. The zones are not obscured uniformly by the knife-edge even if they are chosen very narrow. Shadows enter the zones, one coming from the center and the other from the edge, and they move across at different speeds as the knife-edge is made to cut more and more light. It becomes impossible to determine the correct longitudinal position of the knife-edge with sufficient accuracy.

This difficulty was pointed out—without a solution for it being given—37 years ago in a paper[2] constituting a great contribution to the theory of testing mirrors but seldom mentioned in the literature. This paper was brought to my attention after we had analyzed and solved the problem in a general way. The solution is given in a subsequent paper.* It consists in measuring not at the so-called "center of curvature," that is, at the zone of intersection of pairs of symmetrical light beams upon the optical axis—zone called center of least confusion—but at the real center of curvature of each single zone, that is, at the caustic of the optical system. The new method of measurement can be applied generally and permits the attainment of highest precision.

Conclusion

Combining the arrangement described in this paper with the general method of surveying optical surfaces or systems explained in the article referred to* it is possible to measure a Cassegrain mirror with errors of less than a hundredth of a wave-length of light per zone. This is the precision required for the Cassegrains of large telescopes.

The new method can be applied to any convex surface. It permits the control of spherical as well as aspherical lens surfaces independently of the aberrations introduced by the glass of which the lens is made.

Details of the testing and refiguring of the Cassegrain of the 82-cm La Plata reflector will be published elsewhere. The corrected Cassegrain has been in use since August 1937.

[2] F. L. O. Wadsworth, Popular Astronomy **10**, 337 (1902).

* "On the Errors of Testing and a New Method for Surveying Optical Surfaces and Systems," Ricardo Platzeck and E. Gaviola, J. Opt. Soc. Am. **29**, 484 (1939).

On the Errors of Testing and a New Method for Surveying Optical Surfaces and Systems

RICARDO PLATZECK
La Plata Observatory

AND

E. GAVIOLA
Córdoba Observatory, Argentina

(Received August 31, 1939)

A systematic study of the precision required and of the errors committed in testing parabolic mirrors by the longitudinal aberration and by the transversal aberration methods is made, showing that these methods do not possess in general the necessary accuracy of a hundredth of a wave-length per zone. A new method is developed, which consists in determining the *caustic* or line of the centers of curvature of the surface elements. With this method, a precision of better than a hundredth of a wave-length per zone can easily be obtained. The zones can be comparatively wide. Secondary zones and surface detail can be detected just as well, or even better than by using a plane mirror in conjunction with the parabolic. The use of master flats is thus superfluous. The experimental procedure is explained and results of actual tests are given. By using a thin wire instead of a knife-edge systematic errors are avoided and higher precision is obtained. The caustic method can be applied to the quantitative test of convex surfaces, like Cassegrain mirrors, to the determination of astigmatism, to the study of single lenses, lens systems, Schmidt correcting plates, etc. Its accuracy does not depend on the value of the aberrations, so that surfaces departing considerably from a sphere can be tested just as well as spherical surfaces. It will thus be possible to figure such surfaces with high precision.

"SOMETIME ago my attention was called to the apparent confusion of ideas on the part of different opticians regarding the application of the Foucault method to the testing of the figure of a parabolic mirror at the center of curvature by determining what is commonly termed the 'longitudinal aberration' of the figured surface at this point." Thus reads the beginning sentence of a paper which appeared in 1902.[1] The same thing can be repeated today. The only difference introduced by 37 years is that there is today less confusion as to the actual value of the "longitudinal aberration," but more regarding the accuracy that can be expected from the different methods of surveying an optical surface. Some authors consider that Foucault's method is "only qualitative"; others that its precision cannot surpass $\frac{1}{8}$ of a wave-length of light; others again believe that they can obtain with it the "curve of shape" of the surface committing errors not larger than a few hundredths of a wave-length. Some state that working at the focus, in autocollimation with a master flat, is more precise than measuring at the "center of curvature"; others believe the contrary. Many astronomers believe the method of Hartmann to be "quantitative" and superior to Foucault's; professional opticians on the other hand practically never use the first because they doubt its accuracy. In some optical shops flats are tested exclusively by interference fringes, in others the reliability of this method is doubted and auxiliary spherical concave mirrors, with the flats at 45° and knife-edge near the center of curvature are used. Contradictory statements are also made regarding Ronchi's method.

Now, a knowledge of the accuracy of testing methods is important, not only in order to know the precision with which the actual shape of a finished optical surface or optical system can be determined, but more so because the testing accuracy is the limit of the working accuracy. A surface can be made as accurate and only as accurate as it can be tested. Errors that cannot be seen or measured cannot be corrected. An increase in the precision of testing means an increase in the precision of figuring.

The purpose of the present paper is to contribute to a systematic study of the errors of testing. This study has led us to the use of a new method of surveying optical surfaces or

[1] F. L. O. Wadsworth, Popular Astronomy **10**, 337 (1902).

systems, which possesses higher accuracy and has a wider field of application.

Precision Required

As is well known, mirrors have to be figured four times more precise than lens surfaces. We will consider therefore the accuracy required in mirrors.

Lord Rayleigh has shown that the quality of the optical image of a star begins to be practically affected if the light forming it contains phase differences of $\lambda/4$ (a quarter of a wave-length). If the image is formed, for instance, by a parabolic mirror alone, at its principal focus, the error tolerable in the mirror is therefore $\lambda/8$. If the telescope makes use of two auxiliary mirrors, a Cassegrain and a diagonal, finished with equal precision, the tolerance is decreased to $\lambda/8\sqrt{3}=\lambda/14$. While testing the mirrors zonal screens are used. Let us suppose that, for a large mirror, we have the surface divided in 16 zones of equal weight; the error tolerable per zone is than $\lambda/14\sqrt{16}=\lambda/56$, if the zonal errors are of an accidental nature. If they are systematic the tolerance will be reduced to $\lambda/14\cdot 16=\lambda/224$. Let us adopt as tolerance for one zone $\lambda/100$, and let us try to make the systematic errors as harmless as possible. Since $\lambda/100$ is a small quantity, the

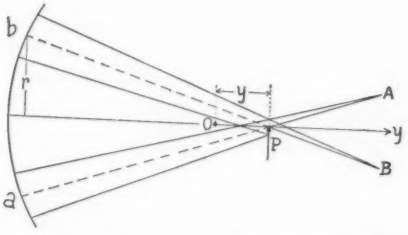

Fig. 1. Testing along the axis at the so-called center of curvature. When slit and knife-edge are at the crossing of the beams the real images of the slit are farther away.

question arises: Can the testing methods give this precision per zone, and if so, under what conditions?

The Longitudinal Aberration Method

Let us suppose that we are surveying a parabolic mirror using a knife-edge apparatus in which the parallax has been eliminated,.i.e., in which the virtual artificial star, or slit, coincides with the knife-edge and these two are always moved together.[2] We have to find, for a pair of symmetrical zones a and b (Fig. 1), the point P at which the normals at the centers of the said zones cross upon the axis. This is not simple, for the point P is not at the center of curvature of either of the two zones, as is tacitly and wrongly assumed frequently,[1] but nearer to them, and therefore the images of the illuminated pinhole

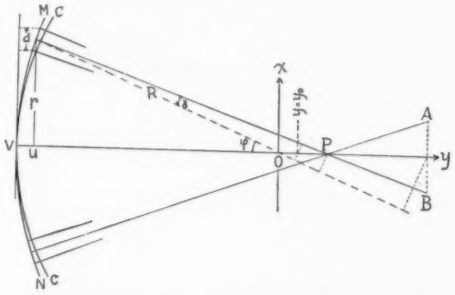

Fig. 2. The geometry of testing a parabolic mirror.

formed by the zones a and b will be farther away, at A and B. The eye placed behind the knife-edge will see the left half of the two zones in shadow and the right half brightly illuminated. In praxis we do not know in advance where P is. We have to find it by observing at which position of pinhole and knife-edge along the optical axis the two shadows entering from the left reach the center of the zones at the same time. This is made still more difficult by the fact that the two shadows move with different speeds. The shadow entering zone a from the periphery moves slowly at first and faster afterwards, while the one entering zone b and coming from the center moves fast at first and slow afterwards. If the center of the zone is not correctly appreciated, then an error in y is committed, because y is a function of r. Now which is the tolerance regarding the appreciation of r? In Fig. 2, let light source and knife-edge lie at P, which is the crossing point of the normals to the parabolic mirror MVN at the center of the pair of zones of width d and mean radius r. What we want to determine

[2] This assumption is made only for the purpose of simplifying the drawings and calculations. In actual practice it is in some cases advantageous to keep the light source fixed. In these cases the aberrations measured are twice the value indicated in the text.

is the actual shape of the mirror MVN referred to a certain theoretical surface. Let us refer it for the moment to the sphere that is tangent to the paraboloid at its vertex V, the center of which is indicated by 0. Now if γ is the angle between the normal to the paraboloid and the normal to the sphere, then the increment in distance between the two surfaces across the zone of width d is $-h=\gamma d$. Now $\gamma(R+y\cos\varphi)=y\sin\varphi$ where $y=\langle OP\rangle_{Nu}$ is the longitudinal aberration of the zone of radius r, and $\sin\varphi=r/R$. As $\cos\varphi\sim 1$ we can write

$$-h=y\sin\varphi d/(R+y\cos\varphi)=yrd/R(R+y). \quad (1)$$

Now y can be neglected against R, if it is smaller than the tolerance δR, which is the case if the surface to be surveyed does not depart greatly from the sphere of reference. If we neglect y, we can write

$$-h=yrdR^{-2}. \quad (1')$$

This h is the magnitude that we want to determine with an error of no more than $\lambda/100$.

Now, accidental errors depend on the magnitude actually measured, which is y. The errors in the determination of r, the mean radius of the screen zone, d its width, and R are systematic errors. Let us consider first the accidental errors. We can write $-h=cy$, where $c=rdR^{-2}$. If we designate the errors in y and in h by δy and δh we have $\delta h=c\delta y=c(\partial y/\partial r)\delta r$. Then the accidental error affecting y comes from its dependence on r. For a paraboloid it is $y=\text{const.}+r^2/2R$ and $\partial y/\partial r=r/R$, which is maximum for the periphery of the mirror.

We have then $\delta h=cr\delta r/R=r^2d\delta r/R^3$ or

$$\delta r=\delta h\cdot R^3/r^2d. \quad (2)$$

Now the tolerance $\delta h=\lambda/100=5.6\cdot 10^{-7}$ cm. The tolerance δr can be made larger by choosing the width d of the zone smaller, but there is a limit set by the bright appearance of the edges of the screen. The practical width of the zone depends also on the distance R from which it is observed. Many observers will find that $d=R/300$ is a fair lower limit, others with very good eyes can go as far as $d=R/600$. Let us set then the first value in (2) and let us call $R/r=4m$, where m is the aperture ratio for the considered zone. We find then

$$\delta r=\delta h\cdot 4800\ m^2=2.7\ m^2\cdot 10^{-3}\text{ cm}. \quad (3)$$

This tolerance is given numerically in column 4 of Table I for different values of m. For an $f:3.3$ mirror the tolerance comes near to 3/10 mm. If $R=3300$ cm for that mirror then the width of the zone that can be well seen is $R/300=11$ cm. and the limit $R/600=5.5$ cm. Now it is easy to see that it is impossible to judge with a precision of 3/10 mm for which value of y the shadows reach at the same time the centers of two symmetrical zones of 11 or 5.5 cm width. To judge the position of the center with the required accuracy, the width of the zone should not surpass 6 or 7 times the tolerance in r. That is $R/300\leqslant 7\delta r$, or $R\leqslant 2100\delta r$. This means that the maximum diameter of a mirror that can be measured with a precision of $\lambda/100$ up to the edge by this method of direct observation is $2r\leqslant 1050\delta r m^{-1}$, which for $m=8$ gives 22 cm, and for $m=3$ only 8.4 cm. This appears discouraging.

Let us now consider the other errors affecting y. For precise measurements y will be read with the help of a micrometer screw and a divided drum. We have then the systematic errors of the screw and the casual errors of reading the drum. What is the tolerance for these?

$$\delta y=\delta h/c'=\delta hR^2/rd$$
$$=1200m\delta h=6.7m\cdot 10^{-4}\text{ cm} \quad (4)$$

for $\delta h=\lambda/100$ as before. The corresponding

TABLE I. *Numerical values of the tolerances in the appreciation of the zonal radius for the longitudinal aberration, transversal aberration and caustic method, breadth of the zones, screw tolerance and width of the diffraction images for different values of the relative aperture m, the half-diameter r and the radius of curvature R.*

1	2	3	4	5	6	7	8	9
m	r	R	δr long.	δr transv.	δr caustic	Δr	δy	$a=2.44\lambda R/\Delta r$
	cm	cm	10^{-2} cm	10^{-2} cm	cm	cm	10^{-3} cm	10^{-2} cm
3.3	250	3300	2.9	2.3	2.2	14.9	2.2	3.01
3.3	100	1320	2.9	2.3	1.4	8.1	2.2	2.2
3.3	50	660	2.9	2.3	1.0	5.1	2.2	1.8
3.3	25	330	2.9	2.3	0.7	3.2	2.2	1.4
4	250	4000	4.3	3.4	2.7	18.1	2.7	3.0
4	100	1600	4.3	3.4	1.7	9.8	2.7	2.2
4	50	800	4.3	3.4	1.2	6.2	2.7	1.8
4	25	400	4.3	3.4	0.8	3.9	2.7	1.4
6	250	6000	9.7	7.7	4.0	27.2	4.0	3.0
6	100	2400	9.7	7.7	2.5	14.7	4.0	2.2
6	50	1200	9.7	7.7	1.8	9.3	4.0	1.8
6	25	600	9.7	7.7	1 3	5.9	4.0	1.4
8	250	8000	17.2	13.8	5.4	36.2	5.4	3.0
8	100	3200	17.2	13.8	3.4	19.7	5.4	2.2
8	50	1600	17.2	13.8	2.4	12.4	5.4	1.8
8	25	800	17.2	13.8	1.7	7.8	5.4	1.4
12	250	12000	38.8	31.0	8.0	54.3	8.1	3.0
12	100	4800	38.8	31.0	5.1	29.5	8.1	2.2
12	50	2400	38.8	31.0	3.6	18.6	8.1	1.8
12	25	1200	38.8	31.0	2.5	11.7	8.1	1.4

values for various m are indicated in column 8 of the Table I. We see there that even for $m=3.3$ the precision required is only about 2 hundredths of a millimeter, which is easy to obtain even with a common screw. The accidental error of reading the drum can be completely neglected.

We will consider now the systematic errors due to the determination of the mean radius of the screen zone. From (1′) we obtain

$$\delta r = \delta h R^2/yd = \delta h \cdot 2R^3/r^2 d, \qquad (5)$$

which is double the tolerance (2) for the accidental error in r. This precision is not difficult to obtain.

We need finally to know the tolerance in the determination of the radius of curvature of the central zone R. From Eq. (1′) we have

$$\delta h = (\partial h/\partial R)\delta R = 2yrdR^{-3}\delta R \qquad (6)$$

and putting $y=r^2/2R$, $R/d=300$, $\delta h=5.6\cdot 10^{-7}$ and $R/r=4m$ we obtain

$$\delta R = 1.1 m^3 \cdot 10^{-2} \text{ cm.} \qquad (6')$$

For $m=3.3$, $\delta R=0.4$ cm. This requirement is not difficult to meet. The tolerance grows fast with the m value: for $m=8$ it is already $\delta R=5.6$ cm. This tolerance is considerably increased if we refer the actual paraboloid to the theoretical surface and not to the sphere as was assumed in Eq. (6). If we put for y the difference between the measured and the theoretical longitudinal aberration $y=y_m-y_t$, then the coefficient of δR is reduced at least 30 times for a fair surface and the tolerance in R is increased in the same proportion.

We have still another question to answer: When can y be neglected against R in (1)? The answer is similar to the former one. Let us call $R+y=S$ for a second and write $\delta h=\delta s yrd/RS^2$. Setting $y=r^2/2R=r/8m$, and writing R^2 for S^2 again we obtain

$$\delta s = 3.1 m^3 \cdot 10^{-2} \text{ cm.}$$

We can neglect y against R if $y \leqslant \delta s$, that is, if $y/\delta s \leqslant 1$. It is $y/\delta s = 4rm^{-4} \leqslant 1$ and

$$2r \leqslant \tfrac{1}{2} m^4 \text{ cm.} \qquad (6'')$$

For $m=3, 4, 5, 6, \cdots$ we find $2r=40, 128, 312, 650, \cdots$ cm as limiting diameters. In these cases y can be neglected in $R+y$ and Eq. (1′) is correct even for a $\lambda/100$ accuracy.

FIG. 3. Photographic determination of the radius of a zone for a given value of the longitudinal aberration using a thin wire instead of a knife-edge.

As the end result of the analysis we find that the weakness of the longitudinal aberration method, as it is usually employed, lies in the difficulty of appreciating correctly the position of the light-shadow limits upon the zones of the screen.

WAYS OF IMPROVING THE LONGITUDINAL ABERRATION METHOD

Two possible ways occur to one at first: (1) to use an observing telescope instead of the naked eye behind the knife-edge; and (2) to eliminate the zonal screen with its disturbing bright contours and place a scale directly on the glass or near to it, on which the values of r would be measured. If one tries them, one finds soon that they do not help much. The reason is that the tolerance in r is large when $\partial y/\partial r$ is small, but then the limit between light and shadow is badly defined and no accurate reading of r can be made even with a good telescope. If $\partial y/\partial r$ is large, the limit light-shadow is better defined, but then the tolerance in r is smaller. The thing to do then is to get a better definition of the light-shadow limit. A single knife-edge has the disadvantage of not being symmetrical. Systematic errors can easily be committed. If one uses two knife-edges that cut the light simultaneously in opposite directions, these systematic errors can be eliminated. This can be accomplished in two ways: by using a slit and by using a thin wire instead of the knife. Figs. 3 and 4 show the appearance of the illuminated field in the two

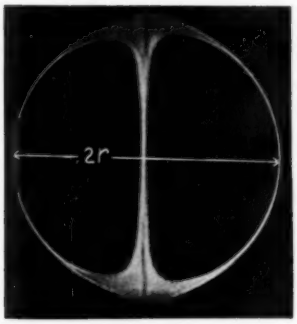

FIG. 4. The use of a thin slit instead of a knife-edge for the better determination of the radius of a zone for a given value of the longitudinal aberration.

cases. The two photographs were obtained by placing a camera behind the double knife-edge. In the case of the thin wire, the camera has to have a lens to avoid double images. In the case of the slit the lens can be eliminated with advantage. The optical system surveyed in this case was a single crown lens of 21.5 cm diameter mounted in autocollimation in front of a plane mirror. Monochromatic light, the blue line of mercury, was used. The way of measuring consists in placing the slit or wire for a certain value of the longitudinal aberration y in such a way that the figure obtained is approximately symmetrical. The distance $2r$ between the zones on the left and right has then to be measured. This is best done on the photograph itself. Repeating the operation for a certain number of y values, one has the function $y(r)$. As long as $\partial y/\partial r$ is comparatively large the method can be used with sufficient accuracy, using the appropriate thickness of the wire or separation of the slit. But as $\partial y/\partial r$ becomes smaller the width of the shadows of the wire or of the corresponding bright zones where light passes the slit become larger and the accuracy is lost. This is shown in Fig. 5, which is a superposition of pictures taken with the same slit for 6 different values of y. For small values of $\partial y/\partial r$ i.e., for the central zones of parabolic mirrors the method becomes inapplicable. But, on the other hand, for these zones the traditional zonal method can be used with sufficient accuracy, so that the two can be considered as complementing each other. To have to use two methods for measuring accurately the whole of a surface is, of course, unsatisfactory.

THE TRANSVERSAL ABERRATION METHOD

In this method,[3] pinhole and knife-edge are placed at a definite constant value of y, for instance $y=y_0$ (see Fig. 2), and moved transversely, parallel to the x axis. Instead of a screen, a scale, for instance an Everest scale, is placed across the mirror. One measures the values of the displacements x corresponding to the positions r of the limit between light and shadow on the surface of the mirror. Instead of a knife-edge a slit or a thin wire can be used.

Now, the increment h of a zone d of mean radius r will be given by

$$-h=(x\cos\varphi+y_0\sin\varphi)d/(R+y_0\cos\varphi). \quad (7)$$

If we set $\sin\varphi=r/R$ and $\cos\varphi=1$, we have

$$-h=(x+y_0r/R)d/(R+y_0). \quad (7')$$

The value of y_0 for which the transversal aberration is measured is arbitrary. The corresponding theoretical value of x is

$$x=r^3/2R^2-y_0r/R. \quad (8)$$

If we want to refer the measured surface to the sphere, we use for x in (7′) the measured transversal aberrations. If we desire to use the theoretical paraboloid as a surface of reference, we subtract from the measured values the theoretical aberrations given by Eq. (8) and we use the difference in Eq. (7′).

Let us analyze the errors and tolerances of this method. The tolerance in r is given by

$$\delta h=\delta r(\partial x/\partial r)d/(R+y_0).$$

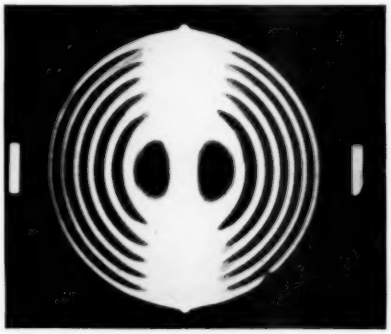

FIG. 5. Showing the limitation of the use of a thin slit: at the center the zones become too wide for accurate measurements. The same occurs using a thin wire along the optical axis.

[3] E. Gaviola, J. Opt. Soc. Am. **26**, 163 (1936).

From Eq. (8) we obtain $\partial x/\partial r=(3r^2-2y_0R)/2R^2$, and we have then

$$\delta r=\delta h 2R^2(R+y_0)/(3r^2-2y_0R)d. \qquad (9)$$

Setting as before $\delta h=\lambda/100=5.6\cdot10^{-7}$ cm, $d=(R+y_0)/300$, $R/r=4m$, calling r_0 the value of r at the edge and choosing $y_0=r_0^2/4R$, we find for the outer zone,

$$\delta r=2.15m^2\cdot10^{-3}\text{ cm}. \qquad (10)$$

Comparing this with (3) we see that the tolerance is now a little smaller than in the previous case. This depends on the value y_0 chosen for the transversal survey.

In the column 5 of Table I the values (10) are given for different relative apertures m.

Let us calculate now the tolerance in the determination of x itself. It is $\delta h=\delta x d/(R+y_0)$ and

$$\delta x=\delta h(R+y_0)d^{-1}=1.7\cdot10^{-4}\text{ cm}, \qquad (11)$$

if we set for δh and d the same values as before.

It is interesting to note that the tolerance δx is constant under the assumptions made. It does not depend on size or relative aperture of the mirror.

Now 1.7 microns is a small distance, but it can be securely determined with a good micrometer screw, and proper methods of measurement. The required precision in r, on the other hand, can be attained for large values of $\partial x/\partial r$ by using slit or thin wire instead of knife-edge, as we have seen before, but not for small values of $\partial x/\partial r$. This method, then, that is useful for local surveys and for surfaces without central symmetry, is unsatisfactory for a high precision survey of a parabolic mirror.

Looking for a New Method

The weakness of the longitudinal and transversal aberration methods is the small tolerance δr. We have to find ways of increasing this tolerance. Now, if we reconsider Eq. (9), we notice that for $r=\pm(\frac{2}{3}y_0R)^{\frac{1}{2}}$ we obtain $\delta r\to\infty$, that is, the tolerance grows to infinity in first approximation. This is a quality of the points $y_0=r_0^2/4R$ and $x=\mp r_0^3/6\sqrt{6}R^2$. A little analysis shows that these two points are the *centers of curvature* of the two zones $r=\pm r_0/\sqrt{6}$, and that they fall on what we may call the *caustic* of the parabolic surface. For each positive value of y_0 we can find two such points. They are the intersection of $y_0=$constant and the caustic.

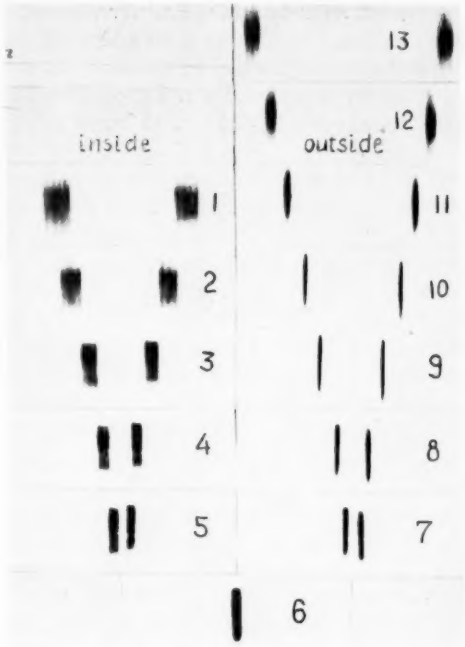

FIG. 6. Images of a thin slit formed by two symmetrical zones of a parabolic mirror before, at and after the crossing upon the optical axis. The images are sharp beyond the crossing point, at the caustic and not at the axis. Notice the diffraction structure of the images inside and outside focus.

If we look again at Fig. 1 we see that if we move pinhole and knife-edge from P along the normal to the center of zone b towards the conjugate image B of the pinhole, formed by that zone, we come to a point where pinhole, knife-edge and conjugate image coincide. At this point, when the knife-edge cuts the light coming from zone b a uniform decrease in intensity over the whole zone will be observed. The main trouble encountered before, the shadow entering the zone from one side, disappears at that point, even if the surveyed surface departs greatly from the sphere.

Figure 6 gives a photographic illustration. It contains a series of photographs of the "images" of a slit formed by two symmetrical zones of a parabolic mirror. The mirror used was a small $m=3$ (diameter 15 cm, focal distance 45.4 cm) made for a large field telescope of the Córdoba

Observatory. The face of the mirror was covered with a screen leaving two symmetrical zones of elliptical shape exposed. The mean radius of the pair of zones was $r=5.5$ cm. They had a width $d=2$ cm and a height of 3 cm. As "artificial star" a slit of 0.04 mm width and 1 mm length was used. Instead of the knife-edge, a photographic plate was put in its place. Plate and illuminated slit were moved together. Each exposure lasted about 10 seconds. The plate was vertically displaced in its own plane between exposures to avoid superposition of the images. The series was obtained displacing slit and plate along the optical axis by 0.81 mm each time from exposures 4 to 8 and by double that amount for the others. Picture 1 was taken 6.5 mm nearer to the mirror than the crossing of the beams. It is then a double "inside focus image" of the slit. Two things can be noticed, the fringe structure of the images, caused by interference, and the lack of symmetry. This last is due to asymmetry in the slit itself. The two slit jaws are in a plane that is not perpendicular to the optical axis. Seen from one of the two zones the slit appears wider than from the other. This is a defect of construction that shows itself markedly here. Notice especially that in picture 4 the left image has a light maximum at the center, while the right one has a minimum.

Picture 13 was taken 9.7 mm beyond the crossing point. It is an "outside focus" image.

The important thing to notice is that when the beams cross upon the optical axis, picture 6, they are not sharp; they are still "inside focus." The focal plane of the images lies at picture 9, some 2.4 mm beyond the crossing point. This is the place of the centers of curvature of the two zones. The use of the words measurement "at the center of curvature" when longitudinal aberrations along the optical axis are determined is incorrect and misleading.

Now, it is clear that accurate measurements can be made only where the images are sharp. They are not so along the optical axis nor for an "arbitrary" plane $y=y_0=$constant. They are sharp along the line of the real centers of curvature, which we will call the caustic, of the surveyed surface. Only along the caustic then, can high precision measurements be hoped to be made.

The Caustic Method. General Formula

The new method consists in determining empirically the caustic curve and calculating from it the figure or curve of shape of the surveyed surface.

Before applying it experimentally, let us determine the value of the errors and tolerances proper to this new method.

Let us suppose that B in Fig. 2 is a point of the caustic, that it is the center of curvature of the right-hand part of the zone of mean radius r and width d. The increment in distance between the surface surveyed and the sphere of reference is $-h=\gamma d$ as before. Now $\gamma(R+y\cos\varphi)=y\sin\varphi+x\cos\varphi$, and therefore

$$-h=(y\sin\varphi+x\cos\varphi)d/(R+y\cos\varphi), \quad (12)$$

if we call x and y the coordinates of the point B.

We can see that this is a generalization of the Eqs. (1) and (7). It reduces to (1) for $x=0$ and to (7) for $y=y_0$.

Equation (12) is then the general formula. It is not limited by the condition of B being a center of curvature. It can be applied to any point of the normal to the center of the zone. If we put $\sin\varphi=r/R$ and $\cos\varphi=1$ we can write

$$-h=(yr+xR)d/R(R+y). \quad (12')$$

Errors and Tolerances. Coordinates of the Centers of Curvature

Let us calculate first the tolerance in r. The magnitudes to be measured are x and y as functions of r. We can write then $-h=ay+bx$ where $a=rd/R(R+y)$ and $b=Rd/R(R+y)$ and treat a and b as constants. It is then

$$\delta h=(\partial h/\partial r)\delta r=(a\partial y/\partial r+b\partial x/\partial r)\delta r.$$

In order to carry on we need now the theoretical values of y and x as functions of r for a parabolic mirror. Let $r^2=2Rs$ be the equation of the parabola referred to the apex V as origin of coordinates. The coordinates of the center of curvature of an element (r, s) of the parabola are given by

$$\eta=s-r'(1+r'^2)/r'', \quad \therefore \quad \xi=r+(1+r'^2)/r'', \quad (13)$$

where $r'=dr/ds$. Now $r'=R/r$ and $r''=-R^2/r^3$, therefore

$$\eta=R+3r^2/2R, \quad \therefore \quad \xi=-r^3/R^2.$$

If we bring the origin to 0 (Fig. 2) we have as coordinates of the center of curvature

$$y=3r^2/2R, \quad x=-r^3/R^2. \tag{14}$$

It is interesting to note that y has now a value exactly three times the longitudinal aberration corresponding to the measurement along the optical axis.

We can proceed now with the calculation of the tolerance. It is $\partial y/\partial r=3r/R$ and $\partial x/\partial r=-3r^2/R^2$, therefore

$$\delta h=(3ar/R-3br^2/R^2)\delta r=0,$$

if we set for a, b their values given above. This means that if we consider only the first differential, the tolerance appears infinite. This should not surprise us because it is, in a way, the definition of the center of curvature.

Let us go a step further

$$\delta^2 h=\tfrac{1}{2}(\partial^2 h/\partial r^2)\delta r^2=\tfrac{1}{2}(a\partial^2 y/\partial r^2+b\partial^2 x/\partial r^2)\delta r^2.$$

If we make the indicated operations and introduce the values of a and b, we find

$$\delta^2 h=\delta r^2 3rd/2R^2(R+y)$$

and if we set as before $R+y=300d$, $R=4mr$ and $\delta^2 h=\lambda/100=5.6\cdot 10^{-7}$ cm we obtain

$$\delta r=2.1(mR)^{\frac{1}{2}}10^{-2} \text{ cm}. \tag{15}$$

The terms of higher order can be neglected. The tolerance depends now not only on m but also on R, which is an advantage for large mirrors. Values calculated according to Eq. (15) for various m and R are indicated in column 6 of Table I. We can see that the tolerance, instead of being expressed in hundredths of a cm as before, can be written now in full centimeters. For a $m=3.3$ mirror of $r=250$ cm, the tolerance is now 76 times larger than for the longitudinal aberration method. The main source of error of the previous methods has been eliminated. We can also see that if we choose the width of the zones seven times the tolerance δr they are wider than $R/300$ and therefore easy to observe with the naked eye. We shall calculate independently the breadth of the zones further below.

The tolerance for the errors of the screen and of the readings of y and x are the same as before, since Eq. (12′) reduces to (1′) and (7′) for $x=0$, $y=y_0$, respectively. It is $\delta y=6.7m\ 10^{-4}$ cm and $\delta x=1.7\cdot 10^{-4}$ cm. These tolerances can be satisfied without difficulty by using the methods explained below.

The tolerance for the cutting of the zones of the screen and for measuring their mean radius r is also the same as before. It is $\delta r=5.4m^2\ 10^{-3}$ cm. This gives over half a millimeter for $m=3.3$. The zonal screen has to be cut and measured with a precision of a few tenths of a millimeter for low m values. For $m=8$ the precision required decreases to about 3 mm.

Finally the tolerance for measuring R turns out to be only half of the value we had in the longitudinal aberration method. It is now $\delta R=0.55m^3\ 10^{-2}$ cm if the surface is referred to the sphere. The additive term y in $R+y$ can be neglected in most cases as before, if the surface is referred to the theoretical paraboloid, but in general not if it is measured against the sphere as surface of reference.

Breadth of Screen Zones and Coordinates of the Average Center of Curvature

We want to know how wide the screen zones can be made. The criterion used before of making the breadth of the screen zones 7 times the tolerance δr is purely arbitrary. One can ask if 7, why not 10 times?

We divide the mirror in small zones to the end of being allowed to consider each of them as a spherical element, the radius and the center of curvature of which we determine. We reconstruct then the paraboloid by placing the spherical elements one after the other, drawing each with its proper radius and center of curvature.

If we choose the zones too wide we will make an error in h for each zone and these errors will have, in general, the same sign. They are systematic errors. As we want to keep the error per zone smaller than $\lambda/100$ the limit in the breadth of the screen zone is given then by the size for which the maximal distance from the particular spherical element of reference becomes $\lambda/100$. We shall calculate this size.

As previous question, we have to decide which is the most favorable spherical element to be taken as reference for our parabolic mirror zone. In first approximation it is the element described by the coordinates of the center of curvature of

the middle of the zone. These coordinates have been already calculated (Eq. (14)).

As the size of the parabolic zone grows, the average center of curvature for the whole zone deviates from the one of its middle. Now, the most favorable spherical element is the one whose center coincides with the average center of curvature of the parabolic zone.

Our task is then first, to determine the average center of curvature for a finite parabolic zone. This will define the most favorable spherical element of reference. We have to calculate then the distances Δh between this element and the actual parabolic zone as a function of Δr and to put a limit to the zone when Δh becomes $\lambda/100$.

Average Center of Curvature

As the average center of curvature will be close to the one of the middle of the zone, we need calculate only a correction to the coordinates $y=3r^2/2R$ and $x=-r^3/R^2$ of the last. The displacement of the center of curvature for a corresponding displacement δr of the surface element will be given by

$$\begin{aligned}\delta y&=\delta r 3r/R+\delta r^2 3/2R+\cdots,\\ \delta x&=-\delta r 3r^2/R^2-\delta r^2 3r/R^2-\cdots.\end{aligned}\tag{16}$$

But what we want to know is the average displacement for all the elements of a wide symmetrical zone. Let us divide the zone into $2n$ elements. The displacement corresponding to the middle of each element will be

$$\pm\delta r=\pm\Delta r(i-\tfrac{1}{2})/2n,\quad i=1,\,2,\,\cdots n.$$

If we call Δr the breadth of the whole large zone.

The corresponding variations of the coordinates are

$$\begin{aligned}\delta y&=\pm\Delta r(i-\tfrac{1}{2})3r/2nR\\ &\qquad+(\Delta r(i-\tfrac{1}{2})/2n)^2 3/2R\pm\cdots,\\ \delta x&=\mp\Delta r(i-\tfrac{1}{2})3r^2/2nR^2\\ &\qquad-(\Delta r(i-\tfrac{1}{2})/2n)^2 3r/R^2\mp\cdots.\end{aligned}$$

If we take now the average over the $2n$ zonal elements, the linear terms disappear and we have

$$\overline{\delta y}=\delta y_c=(3\Delta r^2/8R)\frac{1}{n^2}\sum_1^n(i-\tfrac{1}{2})^2,$$

$$\overline{\delta x}=\delta x_c=-(3r\Delta r^2/4R^2)\frac{1}{n^2}\sum(i-\tfrac{1}{2})^2.$$

Now

$$\frac{1}{n^3}\sum_1^n(i-\tfrac{1}{2})^2=(1+1/n)(2+1/n)/6-(1+1/n)/n-1/4n^2=\lim_{n\to\infty}\tfrac{1}{3}.$$

The corrections for the coordinates of the center of curvature for a finite zone of width Δr are then

$$\delta y_c=\Delta r^2/8R,\quad \delta x_c=-\Delta r^2 r/4R^2\tag{17}$$

and the coordinates themselves

$$\begin{aligned}&y_c=y+\delta y_c=3r^2/2R+\Delta r^2/8R,\\ \therefore\quad &x_c=x+\delta x_c=-r^3/R^2-\Delta r^2 r/4R^2\cdots.\end{aligned}\tag{18}$$

These are the theoretical values that we will later subtract from the measured coordinates in order to refer the actual surface to the theoretical paraboloid.

Breadth of Zones

We can go now a step further and calculate the separation between the parabolic zone of width Δr and the spherical surface with center in y_c, x_c that touches it at its middle.

To do this we use the integration formula (Eq. (12′)) of the caustic method. For y and for x we have to use the differences between the expressions (16) and the values (17). We have then

$$-h=\int d\delta r[(\delta y-\delta y_c)r+(\delta x-\delta x_c)R]/R(R+y).$$

In this integral r, R, $R+y$ and Δr are constants; the variable of integration is δr and its differential $d\delta r$.

Substituting and simplifying, we obtain

$$h=(r/2R^2(R+y))\int(3\delta r^2-\Delta r^2/4)d\delta r,$$

and integrating

$$h=(r/2R^2(R+y))(\delta r^3-\delta r\Delta r^2/4).\tag{19}$$

If we make the derivative of this expression equal zero we shall find the value of δr for which the maximum occurs. This value is

$$\delta r=\pm\Delta r/2\sqrt{3}.\tag{20}$$

Putting this value into Eq. (19), we have

$$|h|_{\max}=r\Delta r^3/24\sqrt{3}R^2(R+y).$$

This is the quantity that should not surpass $\lambda/100 = 5.6 \cdot 10^{-7}$ cm. The maximum value for the breadth Δr of the zone is then

$$\Delta r^3 = 24\sqrt{3} \cdot 5.6 \cdot 10^{-7} R^2 (R+y)/r.$$

If we put $R = 4mr$ and neglect y on the side of R, we find

$$\Delta r = 4.53 (mR^2)^{\frac{1}{3}} 10^{-2} \text{ cm.} \qquad (21)$$

This breadth is given in column 7 of Table I for various values of m and R. We see that the permissible latitude is larger than $R/300$. The zones can be observed with the naked eye without difficulty.

It is to be noticed that the error introduced by the breadth of the zone is, in general, of a systematic character. If we would choose the zones all of the maximum size consistent with the m value, that is, increasing the width as we go from the periphery to the center, the total error to be expected due to this cause would be $n\lambda/100$, if n is the number of zones. If, on the other hand, we make all the zones equal to the one allowed at the edge, the systematic error will decrease as we move to the center.

Size of the "Artificial Star"

Although a pinhole can be used, it is advantageous to have as "light source" a slit. It gives a more uniform illumination of the whole surface of the mirror, a many times greater intensity and permits a more accurate cutting with the knife-edge or thin wire.

The allowable width of the slit depends on the size of the image of diffraction produced by the zones being used. For a thin slit the breadth of the diffraction image produced by a zone of size Δr at distance R is given by

$$a = 2.44 R\lambda/\Delta r \text{ cm.} \qquad (22)$$

A few numerical values for $\lambda = 5.6 \cdot 10^{-5}$ cm are given in column 9 of Table I.

The width of the slit ought to be such that it does not widen the images unnecessarily. As the images vary from 1.4 to 3 tenths of a millimeter, the slit can have a width varying from 0.5 to $1 \cdot 10^{-1}$ mm.

With modern light sources, ribbon filament lamps, one can get large amounts of light through slits of that size.

One necessary precaution is to keep the image of the slit and the knife-edge or thin wire parallel to each other. This is done by observing both with an eyepiece and correcting if required.

We have already all the elements necessary for measuring a parabolic mirror with a precision of $\lambda/100$ per zone. We will now consider the experimental procedure.

Application of the Caustic Method. Experimental Procedure

Let us forget now most of the preceding mathematical formulations and discussions and keep in mind only a few results.

The first thing to do, if we want to survey a parabolic mirror, is to choose the breadth of the screen zones. For the periphery the maximum size is given in Table I for some values of m and R. If not we can calculate it from Eq. (21). Further towards the center we can use broader zones if we wish as the relation m increases. But this is not advisable as we shall see below. Let us select then a breadth below the allowed size for the periphery and that will go an odd number of times into the diameter.

For instance, if we are dealing with an $m = 4$ mirror of 75 cm radius, the maximum breadth at the edge is 7.8 cm. We choose zones of 6 cm which will go 25 times into 150 cm. We cut now a cardboard screen containing 13 holes of rectangular or elliptical shape of 6 cm width and 10 or 12 cm height, separated by 6 cm from each other. The screen is now placed upon the mirror so that the edges of the extreme holes coincide with the borders of the mirror at the ends of, for instance, the horizontal diameter. The mirror is then ready for a first series of measurements of a central and 6 pairs of symmetrical zones. It is advisable to survey always the whole surface and not only a few narrow zones widely separated. To see the zones distinctly and to avoid confusion of the diffraction images without having to cover up the zones leaving only a pair uncovered at the time, as is often done, we divide the measurement in two series. After the first is done, the screen is displaced 6 cm along the horizontal diameter, without touching the mirror and measuring apparatus, and the new series of 6 symmetrical zones is measured. If there is danger of a change in the distance between mirror and apparatus

while the screen is displaced, it is better to have all 25 holes at once, alternating one of them above the horizontal diameter and the next one below. The central zone is placed in the middle. If necessary some of them can be covered during measurement to avoid confusion.

We need now a Foucault apparatus in which longitudinal and transversal displacements can be measured with micrometer screws. If we are observing a single surface or a system of them placed close together the apparatus may have a small parallax. If we are surveying a system of widely separated surfaces, parallax has to be eliminated by a 45° half-transparent plate. A clean thin cover glass plate will do. We have assumed up to now that "artificial star" and knife-edge move together in order to simplify the calculations and diagrams. In all the cases where parallax can be tolerated one may leave the "artificial star" at rest and displace only the knife-edge. This last procedure is even advantageous, as the displacements are in this case double and the error of measurement can so be halved. The measured magnitudes have then to be divided by 2 before comparing them with the theoretical values or introducing them into the integration formulae.

The Foucault apparatus placed in position and lined up in the usual way, we can proceed to determine the coordinates of the images formed by the mirror zones along the caustic. This can be done in different ways.

For the central zone, we need determine only the position of the image formed by it along the optical axis (y value), in the usual way, seeing when the shadow of the knife-edge or of the thin wire does not enter from the left or from the right. We measure then the distance from this position to the face of the mirror to have R. For the next zone, only one zone of a symmetrical pair is observed at a time, we determine its y coordinate in the same way. If the mirror has central symmetry and the apparatus is properly lined up, the same y coordinate applies to the other member of the pair. We measure then the transversal distance $2x$ between the two images leaving the y coordinate constant. As this distance $2x$ has to be measured with a precision of a couple of microns, a few precautions are necessary. The light source should be turned on at least one hour before measuring to obtain stationary temperature conditions. One ought to make an odd number of readings, repeating always the first, to control and compensate systematic lateral displacements of the apparatus due to deformations of the tables, mirror supports, etc.

The knife-edge turns out to be inappropriate for the accurate determination of $2x$ because of its lack of symmetry. The measurements are easier and many times more exact if one uses a thin wire instead. The diameter of the wire ought to be slightly smaller than the width of the diffraction image. It is best to have several of them of varying diameters mounted parallel to each other and separated by a millimeter or two and to try out which one works best.

There are at least three different ways of observing. (1) One places the eye behind the wire and observes the position of the wire for which the intensity of the zone is a minimum. (2) One uses a 10-mm focal distance eyepiece focused on the wire and observes when the wire cuts the diffraction image symmetrically. (3) One places the eyepiece 10 or 20 cm behind the wire and observes the "out of focus image"—in fact a double image of the mirror zone formed by the light passing at both sides of the wire. The two images are superposed but with a lateral displacement due to diffraction at the borders of the wire, so that one can observe the two separately. When the two have equal intensity the wire is bisecting the diffraction image properly (see Fig. 10 where a small error can still be detected in the position of the wire). This last method is of extraordinary sensitivity, because of its differential nature. The need of an appropriate choice of the diameter of the wire in regard to the width of the image becomes here apparent.

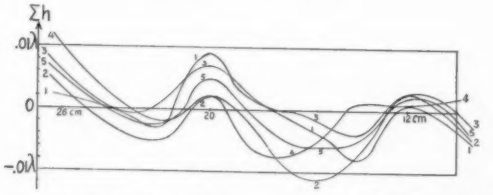

FIG. 7. Five independent measurements of the curve of shape of a part of the 76-cm Córdoba parabolic mirror, using the caustic method and thin wire. The maximum separation of the curves remains within a hundredth of a wave-length of light.

Any one of the three observing ways can be used with sufficient accuracy. The limiting precision will be given (in most cases) by the errors of the screw.

Calculation of the Curve of Shape

Once the coordinates y and x have been determined for all the zones we can proceed to calculate the curve of the mirror. If we want to have it referred to the sphere of radius R we use Eq. (12′) and obtain the increment h for each pair of zones. Σh gives us then the whole curve of shape.

One wants to know, in most cases, the actual curve in regard to the theoretical surface. To obtain this we introduce into Eq. (12′) for y and for x the differences between the measured coordinates and the theoretical values given by (14) or by (18). If the zones of the screen are all of equal size, it is not necessary to use the corrected theoretical values (18), as we shall see presently. The values (14) will do as well. We can now neglect y in $R+y$ in Eq. (12′) in most cases.

Change of the Paraboloid of Reference

For theoretical surface of reference we can use, out of a family of paraboloids of varying radius of curvature R, the one that fits best the actual mirror surface. Now, a small change δR in the radius of curvature will affect primarily only the y coordinate in Eq. (12′). The variation in the integration constants can be neglected. We can write then

$$-h=((y+\delta R)r+xR)d/R^2 \qquad (23)$$

(where y has been neglected in $R+y$) and introduce for y and x the difference between the measured and the theoretical values. We can choose the value of the constant δR so as to obtain the smallest average value of h. This is best found by trying first $\delta R=0$ and then the value that appears appropriate from the inclination of the obtained curve.

It is permissible then, to add a small constant amount to all y values. This changes only the paraboloid of reference.

But (23) can also be written

$$-h=(yr+(x+\delta Rr/R)R)d/R^2. \qquad (24)$$

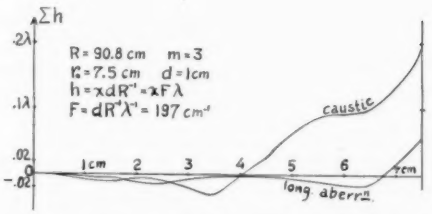

FIG. 8. Two high precision measurements of the same large relative aperture parabolic mirror. The systematic errors of the longitudinal aberration method are demonstrated.

Here a linear function of r appears added to x. A change of surface of reference can also be done then by adding a linear function of r to the x value.

In which way we do the change is arbitrary. We can add a constant amount to the y's or a linear function to the x's or both.

We can see now why it is immaterial to use as theoretical values (14) or (18) if the width of the zones Δr is constant. In this case the corrections (17) are constant for the y values and a linear function of r for the x values. The introduction of the corrections means simply the change of the paraboloid of reference. As we are going to change it afterwards anyhow, in order to select one that fits best our curve, it is immaterial whether we use (14) or (18) as theoretical values. This is true only as long as Δr, the breadth of the zones, is constant. We have here one of the reasons for choosing a constant zonal size. The other one is that the width of the diffraction image remains constant and we can use the same thin wire for all the measurements.

Simplifying Measurement and Calculations

If we know in advance that the actual surface being surveyed lies within a few tenths of a wavelength from the theoretical surface, we can simplify measurement and calculations.

We have seen already that our general formula (12′) is correct not only for the centers of curvature but for any points of the normals to the middle of the zones. If we move away from the caustic what happens is that the diffraction images become unsharp (see Fig. 6) and the tolerance δr and the permissible size of the zones Δr decrease. But as long as we keep near the

caustic no damage is done. Instead of measuring the two coordinates y and x we can then give to the y's in advance the theoretical values and measure only x. Doing so the difference between measured and theoretical value to be set for y in Eq. (12′) becomes zero and we can write

$$-h = xdR^{-1}, \tag{25}$$

neglecting y in $R+y$. For x we have to set the difference between the measured and the theoretical value (14). To this difference we can add an arbitrary linear function of r to choose the best surface of reference. This looks like a reversion to the transversal aberration method but it is not so. Here instead of a constant y_0 we use for each pair of zones a y value that will keep us very close to the caustic.

This simplification can always be used to survey surfaces that fall near a known theoretical curve. Besides paraboloids, spherical mirrors or spherical plane combinations, for instance, can be measured accurately in this way.

The experimental procedure consists in finding first the position of the image formed by the central zone. From this position on we displace the measuring apparatus along the optical axis an amount equal to the theoretical value y for each pair of zones and measure the distance $2x$ between the corresponding diffraction images.

We could also set the apparatus for the theoretical values x and measure the y's, but this is not practical because it is not so easy to obtain the necessary accuracy in y in this way.

Numerical Examples

To see how far the accuracy can be carried under actual shop conditions we made five independent series of measurements of a 30-inch, $m=4$ parabolic mirror of the Córdoba Observatory that has been refigured lately by one of the authors. The method used was to set for the theoretical y values and to measure $2x$ with a thin wire. The screen zones had 2 cm width. For the calculation Eq. (25) was used.

The results are given in Fig. 7. Only a part of the curves is reproduced because as the mirror has errors of the order of $\lambda/10$ near the center and near the border, the figure would become too large if we keep a scale of ordinates that shows appropriately the differences between the five curves of shape. We can see that the maximum separation between any two of the curves does not exceed $\lambda/100$. An average curve could be expected to have still smaller errors, provided there are no systematic errors introduced by the screw.

This example shows conclusively that it is possible to measure a parabolic mirror with a precision better than $\lambda/100$ per zone using the caustic method.

Another interesting example is given by the measurement of the 15-cm, $m=3$ mirror of the Córdoba Observatory. This mirror was figured before the caustic method was developed. It was repeatedly surveyed during figuring by using the longitudinal aberration method with zones 1 cm width. Figuring was considered finished when the curve indicated by longitudinal aberration in Fig. 8 was obtained. The mirror appeared to be good to a hundredth of a wave-length, excepting the last centimeter at the border that was purposely left turned up about 7/100 of a wave-length. The reproduced curve is the result of repeated careful measurements at constant temperature.

After developing the caustic method it was apparent that this curve could not be trusted. In fact, for an $m=3$ mirror of 15 cm radius the

Table II. *Numerical calculation of the curve of shape of an $m=3$ parabolic mirror of 15 cm diameter using the simplified caustic method. The last column gives the results of a measurement of the same mirror by the longitudinal aberration method.*

Zone number	r	y_t	x_t	x_m	$x=x_m-x_t$	$x-0.00013\,r$	h	Σh	Σh
	cm	10^{-3} cm	10^{-4} cm	10^{-4} cm	10^{-4} cm	10^{-4} cm	$\lambda/100$	$\lambda/100$	long. aberr.
1	1	17	1.2	2.0	.8	− .5	−1.0	−1.0	− .5
2	2	69	9.7	12.4	2.7	.1	.2	− .8	−1.2
3	3	149	32.7	35.5	2.8	−1.1	−2.2	−3.0	− .1
4	4	264	77.6	85.7	8.1	2.9	5.7	2.7	− .1
5	5	413	151.5	161.0	9.5	3.0	5.9	8.6	−1.1
6	6	595	262.0	270.5	8.5	0.7	1.4	10.0	−1.8
7	7	809	416.0	430.0	14.0	4.9	9.6	19.6	5.8

FIG. 9a. An $m=4$ parabolic mirror as seen from the "center of curvature" of a peripheral zone. No surface detail is seen. The light fringes are due to diffraction at the edge and at the knife-edge. The picture is a negative.

FIG. 9b. The same mirror observed from the real center of curvature—from a point of the caustic—corresponding to the peripheral zone. Two secondary zones are now plainly visible.

tolerance δr for the center of the peripheral zone is $\delta r = 2.4 \cdot 10^{-2}$ cm if we use the longitudinal aberration method. The width of the zone at the periphery should not have been more than about 6 times δr, that is 1.4 mm. The zones used, as already stated, had a width seven times that tolerable amount. Systematic errors had to be expected near the periphery.

The mirror was afterwards measured with the same zonal screen, but with the caustic method. The tolerable width of the zone at the edge is now 1.3 cm so that the 1-cm zones are now within the tolerance. The curve now obtained is indicated by the word "caustic" in Fig. 8. We see that up to 4 cm from the center the two curves keep close together, but from that point on there is a systematic departure that reaches over $\lambda/10$ at the edge. The systematic errors of the longitudinal aberration method are thus exposed. And the mirror that was thought to be good to $\lambda/100$ turns out to be good only to $\lambda/10$. It will have to be refigured.

The fact that the two curves keep close together to about 4 cm from the center is significant. For that radius the m value has grown already to about 6 and the corresponding δr (see Table I, column 4) nears a whole millimeter. The width of the zone is there 10 times the tolerance and this, on its part, begins to be tolerable. The longitudinal aberration method can be expected to give accurate results from there to the center. And it does.

Systematic errors of the type exposed here are likely to be committed in all longitudinal aberration measurements if the m value is small.

Table II gives an example of how the calculation is made. Column r contains the mean radii of the zones, the next the theoretical values y_t for which the apparatus is set for measuring $2x_m$. The differences $x = x_m - x_t$ if integrated give a curve Σh that mounts too rapidly. To straighten it we subtract from x a linear function of r with $1.3 \cdot 10^{-4}$ cm as coefficient. The new values are then multiplied with the factor $F = d/R\lambda = 197$ cm^{-1} to obtain the increments h directly in wavelengths. The sum of these increments determines the curve of shape. In the last column the curve of shape given by the old longitudinal aberration measurements is numerically indicated. As we see, the calculation is simple enough.

ASTIGMATISM

To detect and measure astigmatism all that is necessary, in general, is to measure the curves of

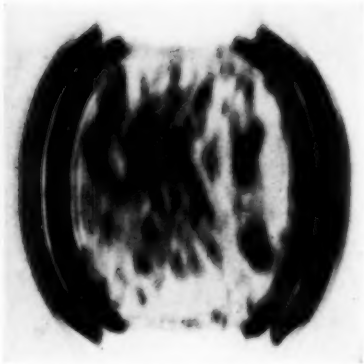

FIG. 10. Surface detail of a bad zone of an $m=4$ parabolic mirror as seen from the caustic using a thin wire instead of a knife-edge. Notice the two directions in which the polishing tool has moved leaving traces of its cutting edges.

shape across two perpendicular diameters. If one wants to make sure that the diameters selected are not the neutral ones, the measurement can be repeated at 45°. An essential condition is that the two perpendicular surveys are referred to the same origin 0. If we add then an arbitrary constant amount to the y's of the zones of one diameter, in order to select the closest paraboloid, the same amount has to be added to the y's corresponding to the other diameter even if the resulting curve is not the best that could be obtained. The same is true for the arbitrary linear function of r that can be added to x.

If the measuring apparatus permits the determination of x horizontally and vertically, be it by rotating slit and thin wire on their own plane, or by rotating the slit, or by changing it, and using a thin wire that bends at right angle in such a way that the two legs of the angle are on the same plane normal to the optical axis, we can make the survey along the two diameters using a double zonal screen with a common central zone. The mirror and screen need not be touched during measurement.

If we cannot measure x in the vertical direction or if the stratification of the air in the measuring room or tunnel makes such impossible, we have to rotate the mirror and measure always horizontally. In this case we observe first the image formed by the central zone alone, using a round pinhole instead of a slit, with an eyepiece and see if it shows any traces of astigmatism. If it does, we measure the longitudinal aberration y of the two linear images in the usual way. Then rotate the mirror until one of them is horizontal. We can now replace the slit instead of the round pinhole and make a complete survey along the horizontal diameter in the usual way. We rotate now the mirror 90° and repeat the survey. When reducing the two to a common origin, we have to remember and take in account the astigmatism of the central zone.

If the central zone does not show astigmatism, then the common origin is immediately given.

The precision with which astigmatism can be detected and measured is the same with which the mirror can be surveyed. If we survey to $\lambda/100$, astigmatism will be known to $\lambda/100$ too.

It is well to remember that astigmatism may be introduced by flexure of the glass.

MASTER FLATS AND SURFACE DETAIL

In Strong's recent book,[4] one can read: "The advantage of testing a parabolic mirror at the focus is evident. The optician works toward a uniform distribution of light over the mirror face. The advantage of testing at the focus over testing *at the center of curvature* is especially great when zones are being removed. Zones which are practically invisible if the mirror is examined *at the center of curvature* become quite conspicuous when it is tested at the focus." (Italics ours.)

This is true if by "at the center of curvature" is meant along the optical axis. If one would observe from the real centers of curvature, along the caustic, the same detail will be seen, for a limited zone at a time, as with a master flat and at the focus. Fig. 9 illustrates the point. They are two Foucault-graphs of the Córdoba 30-inch mirror. In picture (a) the knife-edge is at the optical axis at what is wrongly called "the center of curvature" of a zone near the periphery. No detail can be seen. The light fringe is due to diffraction. In (b) the knife-edge is at the caustic, at the real center of curvature, and a double zone is clearly seen. The zones, after being measured out, were found to have 1 and 2 hundredths of a wave-length in height. The surface detail invisible at the axis is prominent at the caustic. Fig. 9 is reproduced in negative. The spots scat-

[4] John Strong, *Procedures in Experimental Physics*, p. 61–63.

tered irregularly over the surface are false images of light and dark points formed by reflections at the Foucault apparatus sent back by the mirror.

The advantage of the flat is that the whole surface can be surveyed qualitatively at a glance.

The main argument against the use of master flats is that one needs to have them. And they have to be finished with a higher precision than the one expected for the parabolic mirror. And they have to be tested with no less a precision. If the flat is not available and has to be made, one has to figure first a spherical surface, then the flat and then make the spherical parabolic. There are three surfaces to be figured, tested and corrected independently. The amount of work, time and money necessary is about three times the amount demanded by the parabolic mirror itself. The use of the caustic method for testing makes flats superfluous. One can obtain the general curve with higher precision, one reflection against three, and one can detect surface detail and secondary zones equally well; even better if one uses a thin wire instead of a knife-edge. Fig. 10 shows the negative of a bad zone of the 30-inch Córdoba mirror taken during figuring. The diffraction image formed by the zone at the caustic is covered nearly completely by a thin wire. The light passing on both sides of the thin wire forms a double image of the zone in the plate placed 20 cm behind the wire. The two images are displaced against each other laterally. The double image of the bright periphery of the zonal screen, with its diffraction fringes, is strongly shown. If the two are of the same intensity the wire is bisecting the image symmetrically. Here the image on the left is still stronger—count the number of diffraction fringes that can be seen on each side. The wire is perhaps a tenth of a micron off place.

The surface details shown are the traces left by the polishing tool in the last strokes—notice the two dominant directions of the stroke. The height of these "secondary zones" is probably of the order of $\lambda/1000$. The reason why the thin wire gives more detail than the knife-edge is that the first forms two displaced images of complementary character: what is bright in one is dark in the other. The analysis of the surface structure becomes difficult but the local contrast is generally increased.

The Survey of Convex Surfaces

The caustic method can be applied to the high precision survey of Cassegrain mirrors or of any other convex surface by using the experimental arrangement described in the foregoing article. We can do it in two ways:

(1) One determines the coordinates y', x' of the caustic points corresponding to the screen zones of the system Cassegrain+lens (Fig. 1a of former article). One removes the Cassegrain and places a small flat mirror M so that the image formed by the central zone of the screen is in the same place as before and measures the new values y, x of the caustic coordinates. The differences $y'-y$, $x'-x$ brought to the other side of the lens by using the conversion factors $(F_1/F_2)^2$ and (F_1/F_2), respectively, are the coordinates of the caustic of the Cassegrain considered as a concave surface. Subtracting from them the theoretical values

$$y_t = 3e^2r^2/2R, \quad x_t = -e^2r^3/R^2, \tag{26}$$

we introduce the obtained differences into our general formula (12′) and get so the curve of the Cassegrain referred to the theoretical hyperboloid. e is the eccentricity of the hyperboloid.

(2) One measures the system Cassegrain+lens, removes the Cassegrain and places M as before, but on a platform that can be displaced parallel to the optical axis and whose displacements can be measured by screw and drum with a precision δy (see above). For each pair of zones one places now the Foucault apparatus for the y' value obtained before and moves M until the distance $2x$ between the diffraction images is also reproduced. The displacements of M give directly the longitudinal aberration of the Cassegrain. The corresponding theoretical values are given by Eq. (1). The radius of curvature R is given by the distance from the convex surface of the Cassegrain to the surface of the flat in central zone position.

The method explained here for a Cassegrain can be applied to any convex surface, even if it departs considerably from a sphere.

The lens needed for forming an image, if no old one is available, can be made of common plate glass. Its errors are completely eliminated by the measuring procedure.

Conclusion

It is by now clear that the caustic method can be applied to any optical surface or system. One can survey a lens, single or multiple, in front of a flat, a correcting Schmidt plate in front of a spherical concave mirror, etc.

The main advantage of the caustic method is that its precision does not depend on the value of the aberrations of the surveyed system, as in the other methods. If one applies the Hartmann method, for instance, to a system with very small aberrations, spherical mirror at its center of curvature, a good lens system in auto collimation, the obtained precision may be high, because one can place the photographic plates on both sides near the real images formed by the screen zones. But if the system has aberrations this is impossible, and the precision is lost. In the case of Fig. 6, for instance, one could place one plate at position 9 and get sharp images of a pair of zones, but the corresponding "inside focus" plate would be at 3 where the images are very poor. Besides, the images of the other zones would be poor at 9 too. The application of the caustic method will permit the accurate figuring and use of surfaces that depart considerably from the sphere, facilitating the solution of many an optical problem. These surfaces have been avoided up to now because they were difficult to test. The fundamental law of shop optics is that "a surface can be figured as accurately and only as accurately as it can be tested."

It will also be possible to make a quantitative study of the variations in the shape of optical surfaces produced by small temperature gradients.

The study of errors and tolerances has been carried out in detail only for the case of a parabolic mirror in order to deal with a concrete case. The values obtained will not apply to other types of mirrors or to lenses. For lenses the tolerances are in general four times greater, other things being equal. It is easy to calculate the errors and tolerances for any type of surface of known theoretical curve of shape. One needs only put into Eqs. (1), (7) and (12) the corresponding theoretical expressions for y and for x and repeat the calculations as above.

We wish to express our thanks to Mr. Felix Aguilar, director of the La Plata Observatory, and to Mr. Juan José Nissen, director of the Córdoba Observatory, for their support of this work.

Erratum: A Mechanical Integrator for Evaluating the Integral of the Product of Two Functions and its Application to the Computation of I.C.I. Color Specifications from Spectrophotometric Curves

J. A. Van den Akker
The Institute of Paper Chemistry, Appleton, Wisconsin

(J. Opt. Soc. Am. **29**, 364 (1939))

The equations in the first line of the first column on page 369 should read

$$\delta x = (\delta X - (X/S)\delta S)/(S+\delta S)$$

and

$$\delta y = (\delta Y - (Y/S)\delta S)/(S+\delta S),$$

where $S=X+Y+Z$. Since δS enters the corrected equations, it is necessary to measure δZ as well as δX and δY.

Color Tolerance Report Available

REPRINTS of the papers on color tolerances given at the technical session of the last joint meeting with the Inter-Society Color Council (February, 1939) are now available.

Copies have been furnished by the Council to all its delegates and members. As long as the supply lasts other members of the O.S.A. may purchase copies by enclosing fifty cents (stamps of small denominations satisfactory) and addressing requests to: Inter-Society Color Council, P. O. Box 155, Benjamin Franklin Station, Washington, D. C.